c-Myc regulates A-Raf kinase splicing and ERK pathway activation

Jens Rauch[1,2], Kim Moran-Jones[2,3], Valerie Albrecht[4], Thomas Schwarzl[1], Keith Hunter[5], Olivier Gires[6] & Walter Kolch[1]

[1] *Systems Biology Ireland, University College Dublin, Ireland.*

[2] *Beatson Institute for Cancer Research, Garscube Estate, Switchback Road, Glasgow, UK.*

[3] *Garvan Institute of Medical Research, Darlinghurst, NSW, Australia.*

[4] *Department of Neurosurgery, Tumorbiological Laboratory, Ludwig-Maximilians-Universität , Munich, Germany.*

[5] *School of Clinical Dentistry, University of Sheffield, Sheffield, UK.*

[6] *Clinical Cooperation Group Molecular Oncology, Department of Head and Neck Research, Ludwig-Maximilians-Universität München, Munich, Helmholtz Zentrum München, German Research Center for Environmental Health, Munich, Germany.*

Correspondence should be addressed to:

Walter Kolch

Tel.: +353-1-716-6931

e-mail: walter.kolch@ucd.ie

Running Title:

c-Myc regulates A-Raf splicing via hnRNP H

Keywords:

hnRNP H, c-Myc, A-Raf, splicing, MST2, Ras

Abstract

A-Raf can inhibit apoptosis by binding to the pro-apoptotic MST2 kinase. This function is dependent on the expression of hnRNP H, which ensures the correct splicing of the *a-raf* mRNA to produce the full-length protein. Here, we show that expression of hnRNP H and production of full-length A-Raf is positively controlled by c-Myc. Low c-Myc reduces hnRNP H expression and switches *a-raf* splicing to produce A-Raf$_{short}$, a truncated protein, which fails to regulate MST2, but retains the Ras binding domain and functions as a dominant negative mutant suppressing Ras activation and transformation. Human colon and head and neck cancers exhibit high hnRNP H and high c-Myc levels resulting in enhanced A-Raf expression and reduced expression of A-Raf$_{short}$. In normal cells and tissues where c-Myc and hnRNP H are low, A-Raf$_{short}$ suppresses ERK activation suggesting that it acts as a safeguard against oncogenic transformation.

Introduction

The family of Raf protein kinases, which comprises A-Raf, B-Raf, and Raf-1, is at the apex of the three-tiered Raf-MEK-ERK/MAPK pathway that regulates many fundamental cellular functions, including proliferation, differentiation, transformation, apoptosis and metabolism (1). Raf kinase activation is initiated by binding to activated Ras GTPases at the cell membrane, which triggers a complex series of activation events that comprise interactions with proteins and lipids as well as coordinated dephosphorylation and phosphorylation events (2, 3). A-Raf is the least studied member of the Raf kinase family (4). In general, A-Raf seems to be regulated similar to Raf-1, with binding to activated Ras initiating the growth factor induced activation of A-Raf. However, A-Raf is a poor MEK kinase with barely measurable catalytic activity, which is due to unique non-conserved amino acid substitutions in the N-region (5). Independent of kinase activity, A-Raf constitutively binds mammalian sterile 20-like kinase (MST2) and suppresses MST2 activation and induced apoptosis (6).

The ERK pathway is frequently activated in cancer, often due to activating mutations in Ras (7, 8) or B-Raf (9, 10). By contrast, Raf-1 is rarely mutated (11), and to date no oncogenic A-Raf mutations were found. However, elevated A-Raf expression levels have been observed in a number of malignancies including astrocytomas (12), pancreatic ductal carcinoma (13), angioimmunoblastic lymphadenopathies (14), head and neck squamous cell carcinomas, and colon carcinomas (6, 15).

One way to regulate protein expression and activity is alternative splicing. For B-Raf several different splice forms are known. Two variable exons, 8b and 10, allow for the generation of four distinct isoforms (16, 17). While the presence of exon 10 enhances the basal kinase activity and affinity to MEK, exon 8b has the opposite effect (16). Thyroid carcinomas express B-Raf splice variants that lack the N-terminal auto-

inhibitory domain resulting in constitutively active B-Raf variants, suggesting that alternative splicing regulation is a pathophysiological mechanism for oncogenic B-Raf activation (18). An alternative Raf-1 splice form lacking exon 3 was reported in lung cancer, however the functional consequences are unknown (19). Recently, two alternative murine A-Raf splice forms were described, DA-Raf1 and DA-Raf2, which contain the Ras binding domain (RBD) but lack the kinase domain due to pre-terminal stop codons (20, 21). DA-Raf1 and DA-Raf2 bind to activated Ras, but due to the lack of a kinase domain cannot transduce a signal and act as dominant-negative antagonists of the Ras-ERK pathway. Thus, DA-Raf1 is a positive regulator of myogenic differentiation by inhibiting activation of the ERK pathway (20). In another cellular environment, DA-Raf2 binds and colocalizes with the ARF6 GTPase on tubular endosomes and acts as dominant negative effector of endocytic trafficking (21). We recently reported that expression of the full length A-Raf protein requires the expression of the splice factor hnRNP H, which is upregulated in several tumours including colon and head and neck cancers (6, 15) We showed that hnRNP H upregulation ensures the expression of the mature *a-raf* mRNA thus allowing the sufficient production of full-length A-Raf protein to counteract MST2-mediated apoptosis.

Here, we report that *hnRNP H* is a direct transcriptional target of c-Myc, which stimulates its expression. The proto-oncogenic transcription factor c-Myc is a key regulator of various cellular processes such as cell growth, proliferation, apoptosis, and differentiation (22, 23). Recent studies suggest that c-Myc regulates about 15% of all annotated genes by direct transcriptional activation (24, 25). Deregulated and elevated expression of *c-myc* has been shown for a wide range of cancers and it is estimated that c-Myc is involved in 20% of all human cancers (26). We show that hnRNP H maintains the expression of full-length A-Raf protein by suppressing alternative splicing of

the *a-raf* mRNA. This novel splice form, A-Raf$_{short}$, incorporates intronic sequences, and generates a 171 amino acid protein, which lacks the kinase domain. While A-Raf$_{short}$ fails to regulate MST2-mediated apoptosis, it is a potent inhibitor of ERK signaling and cellular transformation by binding and blocking activated Ras. A-Raf$_{short}$ expression levels were reduced in several cancer entities, suggesting that A-Raf$_{short}$ acts like a tumour suppressor protein in these tumours.

Materials and Methods

Cell lines

HeLa, GHD-1, HCT116, and NIH3T3 cells were cultured in standard DMEM containing 10% fetal calf serum (FCS). Cell lines were either purchased from Cancer Research UK or ATCC and were authenticated by the European Collection of Cell Cultures (ECACC). GHD-1 is a self-established cell line from a hypopharynx HNSCC tumour (27).

Transfections

Transient transfections were conducted with Lipofectamine 2000 reagent (Invitrogen, Paisley, UK) or the Nucleofector system (Lonza Cologne, Cologne, Germany) according to the manufacturers' instructions.

Focus Assays

Focus assays were conducted as described previously (28). Briefly, NIH 3T3 cells were transfected with Lipofectamine (Invitrogen) and allowed to grow to confluence. The plates were incubated for 12-15 days. Then, cells were fixed, stained with Giemsa, and the foci were counted.

Semi-quantitative RT-PCR

RNA from human tissues was isolated using the Precellys 24 cell lysis system (Bertin Technologies, Montigny-le-Bretonneux, France). Total RNA from tissues and cell lines was isolated using the RNeasy Mini Kit (Qiagen, Hilden, Germany and cDNA was generated using the SuperScript First-Strand Synthesis System for RT-PCR (Invitrogen, Paisley, UK) according to the manufacturers' instructions.

Immunoprecipitations

Immunoprecipitations were conducted as described previously (6) with the following immobilized antibodies: Monoclonal mouse anti-HA tag antibody 3F10 (Roche Diagnostics, Mannheim, Germany), monoclonal mouse anti-flag antibody M2 (Sigma, Taufkirchen, Germany), polyclonal goat anti-human MST2 antibody sc-6211 (Santa Cruz, Santa Cruz, US), monoclonal mouse anti-human Ras antibody sc-29 (Santa Cruz, Santa Cruz, US).

MST2-kinase activity assay

MST2 kinase activity was measured by in-gel assays as described before (29).

Apoptosis assays

Apoptosis was determined as described previously (6) by measuring subgenomic DNA.

Statistical analysis

Significance levels were determined by two-tailed Student t-test analyses. Due to the non-normal distribution of the expression analysis data (RT-PCR), results are given as the median with the interquartile range (IQR). For comparison of hnRNP H and A-Raf isoform expression between sample groups, we used the Wilcoxon signed-rank test. All tests were two-sided and results considered significant if $p<0.05$.

Results

HnRNP H regulates A-Raf isoform selection

We reported recently, that the splice factor hnRNP H is necessary for the proper expression of the mature A-Raf mRNA (6). Here we show that, when hnRNP H is depleted a novel, alternatively spliced A-Raf mRNA species appears at the expense of the mature mRNA.

Depletion of hnRNP H decreased the levels of mature A-Raf mRNA and full-length protein levels, while causing the appearance of a new mRNA species, which yielded a larger PCR product (Fig. 1A). Sequencing revealed that introns two and four of the *a-raf* gene were included while introns one and three were spliced out (Figure S1 and S2). This alternative *a-raf*$_{short}$ mRNA encodes 171 amino acids that are only partially related to the A-Raf$_{wt}$ protein sequence due to the intronic inclusions. PANTHER database entries for the full-length generic and the alternative mRNAs/proteins are hCT20300/hCP44398 and hCT2257035/hCP1885829, respectively. The cognate A-Raf$_{short}$ protein lacks the C-terminal two-thirds of A-Raf$_{wt}$ including the kinase domain because of the presence of a stop codon at nucleotide position 716 in intron 4 (Fig. S2). Pre-terminated mRNAs are commonly prone to nonsense-mediated decay (32). However, endogenous A-Raf$_{short}$ protein was detectable (Fig. 1B) suggesting a physiological function for A-Raf$_{short}$. Furthermore, downregulation of hnRNP H caused a reduction in the expression of the full length A-Raf$_{wt}$ protein with a concomitant increase in the expression of the A-Raf$_{short}$ protein (Fig. 1B), confirming the results of the mRNA expression at the protein level. Pre-incubation of primary antibodies with the A-Raf$_{short}$ peptide used for immunisation resulted in a complete loss of detection by the A-Raf$_{short}$-, but not by the HA-specific antibody (Fig. 1C).

Alternative splice variants of *a-raf* differ in function

Full-length A-Raf prevents apoptosis by sequestering and inactivating the proapoptotic kinase MST2 (6). In contrast, A-Raf$_{short}$ did not interact with flag-tagged MST2 or endogenous MST2 (Figs. 2A,B). Consequently, A-Raf$_{short}$ was neither able to suppress endogenous MST2 kinase activity (Fig. 2C), nor apoptosis in response to hnRNP H knock-down, as measured by the percentage of cells with a subG1 DNA content, the cleavage of PARP and caspase 3 (Fig. 2D).

A-Raf$_{short}$ negatively regulates the Ras-ERK pathway

The truncated A-Raf$_{short}$ contains the Ras-binding domain (RBD) including novel amino acids derived from intronic sequences but lacks the S/T rich domain and the kinase domain. This structure suggested that A-Raf$_{short}$ might act as dominant-negative Ras antagonist. Overexpression of A-Raf$_{short}$ in HeLa, GHD-1, and HCT116 cancer cells (Fig. 3A), reduced cell numbers (Fig. 3A), possibly by inhibition of Ras-ERK signalling. In serum-stimulated HeLa cells overexpression of A-Raf$_{short}$ leads to a decrease in pERK levels 3-fold while having no effect in quiescent cells (Fig. 3B-C, Fig. 4A). In contrast, phosphorylation levels of Akt were unchanged after A-Raf$_{short}$ overexpression (Fig. 3C) suggesting that A-Raf$_{short}$ selectively antagonizes Ras-ERK signalling leaving Ras-PI3K-Akt signalling unaffected. While increased expression of A-Raf$_{short}$ led to a decrease in ERK activity, depletion of A-Raf$_{short}$ using an isoform-specific siRNA had the opposite effect, i.e. increasing activating phosphorylation levels of ERK (Fig. 3D). In serum-stimulated HeLa cells, knockdown of A-Raf$_{short}$ increased pERK by 30%, while having no effect in quiescent cells (Fig. 3D).

A-Raf$_{short}$ interacts with Ras and antagonises Ras transformation

In order to act as a Ras antagonist, A-Raf$_{short}$ should interact with activated Ras. We transfected HeLa cells with A-Raf$_{short}$ or full length A-Raf (A-Raf$_{WT}$) and performed co-immunoprecipitations showing that both proteins interact with Ras in serum-stimulated cells (Fig. 4A). The same results were obtained with endogenous A-Raf$_{short}$ and Ras (Fig. 4B). Furthermore, experiments where different amounts of A-Raf$_{short}$ and A-Raf$_{WT}$ were co-transfected, showed that A-Raf$_{short}$ efficiently competes with A-Raf$_{WT}$ for binding to activated Ras (Fig. 4C). These data confirm that A-Raf$_{short}$ acts as a physiological negative regulator of Ras-ERK signalling.

Oncogenic Ras is a well-described activator of Ras-mediated ERK signalling and induces transformation in mouse fibroblasts (33, 34). As A-Raf$_{short}$ interacted with activated Ras, and abrogated ERK activation, we asked whether oncogenic Ras-induced transformation was inhibited by A-Raf$_{short}$. NIH3T3 cells were transfected with activated Ras mutants (H-RasV12, K-RasV12, N-RasV12) and co-transfected with A-Raf$_{short}$ and tested for the ability to generate foci of transformed cells (Fig. 4C,D). A-Raf$_{short}$ significantly decreased foci numbers with all three Ras isoforms suggesting that A-Raf$_{short}$ can inhibit transformation by all three Ras members. In order to prove that A-Raf$_{short}$ is acting directly on Ras and not on downstream effectors, NIH3T3 cells were co-transfected with A-Raf$_{short}$ and the viral Raf oncogene (vRaf), which lacks the Ras binding domain and transforms cells independently of Ras (33). A-Raf$_{short}$ had no significant effect on v-Raf induced foci numbers, showing that A-Raf$_{short}$ is inhibiting activated Ras and not the downstream kinase Raf (Fig. S3A, B). We also tested whether the function of A-Raf$_{short}$ differs from other known A-Raf splicing isoforms. In colony formation assays, daRaf1 and daRaf2, like A-Raf$_{short}$, significantly decreased foci numbers with all three Ras isoforms suggesting that these isoforms have overlapping functions (Fig. S3C, D).

c-Myc regulates A-Raf isoform selection via hnRNP H.

hnRNP H is over expressed in several carcinoma entities and regulates *a-raf* splicing (6). We asked therefore, which process is responsible for the expression of hnRNP H. As hnRNP H was found as a target gene of the proto-oncogene c-Myc in microarray experiments (24) we tested this hypothesis experimentally in more detail. Depleting c-Myc from HeLa cells using specific siRNAs reduced hnRNP H protein expression levels and, in parallel, decreased levels of A-Raf$_{WT}$ and increased levels of A-Raf$_{short}$ (Figure 5A). Increased cell confluence triggered a similar response, i.e. decreasing levels of c-Myc, hnRNP H, and A-Raf$_{WT}$ while increasing levels of A-Raf$_{short}$ (Fig. S4). These results suggest that a concerted response of c-Myc, hnRNP H and A-Raf isoform expression is part of the physiological programme how cells respond to different growth conditions. To ascertain that this response was coordinated by c-Myc, we transfected HeLa cells with MycER^{T} (35). MycER^{T} is a chimeric protein where c-Myc is fused to a mutated ligand binding domain of the human estrogen receptor. MycER^{T} is retained in the cytoplasm due to the ER portion binding to Hsp90. Addition of the estrogen analog 4-hydroxytamoxifen (4-OHT) releases MycER^{T} and triggers its translocation to the nucleus and activation of Myc-induced transcription. In the absence of 4-OHT, expression levels of hnRNP H, A-Raf$_{WT}$, and A-Raf$_{short}$ were constant over a timecourse of 8 hrs. Upon addition of 4-OHT, hnRNP H and A-Raf$_{WT}$ levels increased, while A-Raf$_{short}$ expression decreased (Figure 5B). Additional knock-down of hnRNP H using specific siRNAs abrogated this effect indicating that c-Myc is regulating A-Raf isoform selection via control of hnRNP H expression. Endogenous activation of c-Myc by EGF stimulation corroborated these results (Figure 5C). While expression levels of hnRNPH, A-Raf$_{WT}$, and A-Raf$_{short}$ remained stable

in starved cells, activation of c-Myc led to increased hnRNP H and A-Raf$_{WT}$ expression, but decreased A-Raf$_{short}$ expression.

Data from the ENCODE project (31) suggested, that c-Myc binds to three regions in the HNRNPH1 promoter (Fig. S5). We could identify four putative, non-canonical E-Boxes 957bp (CATGTG), 949bp (CACATG), 530bp (CAGCTG), and 63bp (CAGCTG) upstream of the transcription start site, which coincide with the ChIP-Chip data from ENCODE in six different cell lines (Fig. S5). In order to determine direct interaction of c-Myc with the HNRNPH1gene we performed a chromatin immunoprecipitation (ChIP) analysis of the human HNRNPH1 promoter. ChIP indicated that c-Myc was constitutively present at three E-Boxes of the HNRNPH1 promoter region (957bp, 949bp, 530bp) in both serum-starved and stimulated cells. However, c-Myc was recruited to the E-box nearest to the transcription start site only in stimulated cells (Fig. 5D). Collectively, our results show that hnRNP H is a direct target of the proto-oncogene c-Myc and that c-Myc regulates the ERK pathway via hnRNP H and subsequent regulation of A-Raf isoform expression.

The A-Raf$_{short}$ isoform is downregulated in carcinomas.

The expression of the proto-oncogene c-Myc is elevated in a plethora of human tumours (22). Additionally, hnRNPH and A-Raf$_{WT}$ were shown to be overexpressed in several carcinoma entities including head and neck carcinomas and colon carcinomas (6). Therefore, we asked if A-Raf$_{short}$ and other A-Raf isoforms are regulated during carcinogenesis and whether their expression is dependent on the expression of the upstream regulators c-Myc and hnRNP H. To this end, endogenous mRNA expression levels of *c-myc*, *hnrnph*, *a-raf$_{wt}$* , and *a-raf$_{short}$* were analysed in a series of human head and neck carcinomas (T, n=17) and adjacent non-malignant tissues (N, n=14) by semi-quantitative RT-PCR (Fig. 6A). At the single-patient level, a median relative

expression of 2.3-fold for *c-myc*, 1.7-fold for *hnrnph*, 1.5-fold for *a-raf*$_{wt}$, and 0.5-fold for *a-raf*$_{short}$ in tumour specimens was calculated, indicating that *c-myc*, *hnrnph* and *a-raf*$_{wt}$ are over expressed in carcinomas. In contrast, *a-raf*$_{short}$ appears to be downregulated in tumours.

Additionally, after stratifying patients according to their relative expression levels of *c-myc*, *hnRNP H*, *a-raf*$_{wt}$, and *a-raf*$_{short}$ mRNA in tumour tissue, a significant number of patients showed high expression of *c-myc* (χ^2=7.0, p=0.082), *hnRNP H* (χ^2=17.3, p=0.0001) and *a-raf*$_{wt}$ (χ^2=24.1, p=0.0001) in tumours while at the same time showing a significant downregulation of *a-raf*$_{short}$ (χ^2=7.0, p=0.008).

Comparing the relative expression in normal and tumour tissues (Fig. 6B, Table 1) we found that in tumour tissues the expression of *c-myc* (2.5-fold), *hnRNP H* (1.9-fold), and *a-raf*$_{WT}$ (1.3-fold) was significantly higher than in normal tissues. In contrast, *a-raf*$_{short}$ expression in tumours was significantly downregulated compared to normal tissues (1.6-fold decrease). Pearson's correlation (Fig. 6C) showed a significant correlation between *c-myc*/*hnrnph* (r^p=0.8; p<0.001) and *hnrnph/a-raf*$_{wt}$ (r^p=0.7; p<0.009).

Additionally, we assessed endogenous mRNA expression levels of *c-myc* and *a-raf*$_{short}$ in a series of 29 human Dukes B colon carcinomas and autologous adjacent non-malignant tissues by semi-quantitative RT-PCR (Fig. 6B, Table 1). Similar to the results observed in head and neck carcinomas, at the single-patient level a median relative overexpression of 6.4-fold for *c-myc* and 0.85-fold for *a-raf*$_{short}$ was observed in tumour specimens. Furthermore, comparing the relative expression in normal and tumour tissues, *c-myc* expression was significantly higher in tumours than in normal tissue. In contrast, *a-raf*$_{short}$ expression was significantly downregulated in tumours compared to normal. Importantly, we observe similar trends in the corresponding A-

Raf protein isoform levels, in a limited number of autologous tissue samples from head and neck carcinomas (n=3). While A-Raf$_{short}$ protein is downregulated in carcinomas by trend (p=0.08), expression of A-Raf$_{wt}$ prevails in carcinomas (p=0.02) (Fig. S6).

The other two human A-Raf isoforms, daRaf1 and daRaf2, were found to be barely detectable at the mRNA level in the human tissues investigated (semi-quantitative RT-PCR, 1/89 samples, data not shown). Expression of these isoforms was only investigated in mouse tissues and their expression/regulation in human tissues is not known.

Discussion

Alternative splicing occurs in more than 90% of genes (36), and is considered as a key regulatory process by which a common pre-mRNA transcript leads to different mature RNAs, thus producing diverse and even antagonistic functions (37). This greatly expands information content and versatility of the transcriptome generating tissue, stage, and development specific gene expression patterns (38). Tumour suppressors are often inactivated by splicing in cancer, whereas oncogenes are inactivated by alternative splicing during normal differentiation (39, 40). Components of the splicing machinery, such as hnRNP proteins and other RNA binding proteins, have been found altered in tumours and can contribute to cancer cell survival and invasiveness (41).

We showed previously that the splicing factor hnRNP H is overexpressed in colon and head and neck cancers, and promotes the correct splicing of the *a-raf* mRNA that encodes the wildtype full-length A-Raf protein, which binds to and inhibits the pro-

apoptotic kinase MST2 (6). In this previous work we also showed that overexpression of A-Raf$_{WT}$ can overcome the effects of siRNA-mediated knockdown of hnRNP H.

hnRNP H can regulate alternative splicing of Bcl-X (42) and a neuron-specific variant of Src (43). In both cases, hnRNP H binds to G-rich RNA stretches (44), similar to sequences found in the intron sequences included in A-Raf$_{short}$. Although hnRNP H favours the production of the pro-apoptotic Bcl-X$_s$ isoform (42), this splicing event does not prevent the A-Raf mediated rescue from apoptosis resulting from hnRNP H overexpression (6).

A-Raf$_{short}$ differs from DA-Raf1 and 2, which encompasses the uninterrupted RBD and adjacent cysteine rich domain. DA-Raf1 and 2 were not expressed in head and neck tissues and in human colon specimens except for one out of 89 samples (data not shown). This fits the current understanding of alternative splicing as usually only two isoforms of a given number of potential isoforms are predominant at the same time in a given tissue (36). Intron inclusion is a rare event in alternative splicing (36) and, in combination with pre-terminal stop codons, these transcripts are commonly prone to nonsense-mediated decay (32). However, sequence-specific Northern blotting showed that *a-raf$_{short}$* mRNA exists in normal human tissues such as brain, placenta, kidney, pancreas, lung, and spleen (data not shown). The resulting A-Raf$_{short}$ protein is expressed both in cultured cells and in human tissues at low but stable levels, which is consistent with recent findings that such pre-terminated mRNAs typically express low levels of protein (45).

Functionally, A-Raf$_{short}$ inhibits ERK pathway activation by competing for binding to activated Ras. This was un-expected, as intron 2 is inserted into the RBD between glutamine 29 (66 in Raf-1) and lysine 47 (84 in Raf-1), which together with arginine 52 (89 in Raf-1) form a functional epitope in Raf-1 that determines the affinity to Ras

(46). However, the binding of A-Raf$_{short}$ to Ras was GTP dependent and of similar affinity as full-length A-Raf, suggesting a functionally relevant interaction. The functionality of this interaction was corroborated by the finding that A-Raf$_{short}$ behaved as a dominant negative mutant, which suppressed Ras mediated transformation and ERK activation. In contrast, A-Raf$_{short}$ cannot bind to and inhibit MST2 pro-apoptotic signalling. Our finding that the expression of A-Raf$_{short}$ is reduced in cancers correlating with the overexpression of hnRNP H and increased expression of full-length A-Raf protein also suggest that alternative *a-raf* splicing is a pathophysiological mechanism that tumours use to evade apoptosis.

We show that one mechanism regulating hnRNP H levels is via the proto-oncogene c-Myc. As suggested by data from the ENCODE project (31) we show that c-Myc binds directly to a non-canonical E-box in the hnRNP H1 gene promoter in a mitogen-dependent way. Knockdown of c-Myc decreased levels of hnRNP H and subsequent A-Raf$_{short}$ splice form selection. Activation of c-Myc had the opposite effect. Interestingly, c-Myc also stimulates the expression of other members of the hnRNP family, hnRNP A1, hnRNP A2, and hnRNP I (47). These hnRNP proteins promote the alternative splicing of pyruvate kinase resulting in the expression of the embryonic isoform, PKM2, which is almost universally re-expressed in cancer, and stimulates aerobic glycolysis (48). Thus, c-Myc can regulate two splice events via hnRNP proteins that enhance survival via A-Raf mediated MST2 inhibition and switch metabolism to the aerobic glycolysis typical for cancer cells. Additional crosstalk between these two pathways may exist at the protein level as A-Raf was reported to bind to and regulate PKM2 function (49).

In summary, we propose the following working hypothesis (Fig. 6D): In tumour cells high levels of c-Myc elevate expression of the splice factor hnRNP H shifting the balance of *a-raf* mRNA splicing in favour of producing the full-length A-Raf protein, which is crucial to keep pro-apoptotic MST2 signalling in check. In normal cells c-Myc levels are low, resulting in reduced hnRNP H expression and a shift of *a-raf* splicing towards A-Raf$_{short}$ with the dual effect of relieving repression of MST2 and reducing ERK pathway activity due to Ras blockade by A-Raf$_{short}$.

Acknowledgements

This work was supported by Cancer Research UK and Science Foundation Ireland under Grant No. 06/CE/B1129**.**

References

1. Yoon S, Seger R. The extracellular signal-regulated kinase: multiple substrates regulate diverse cellular functions. Growth Factors 2006; 24: 21-44.

2. Wellbrock C, Karasarides M, Marais R. The RAF proteins take centre stage. Nat Rev Mol Cell Biol 2004; 5: 875-85.

3. Dhillon AS, Hagan S, Rath O, Kolch W. MAP kinase signalling pathways in cancer. Oncogene 2007; 26: 3279-90.

4. Rauch J, Kolch W. A-Raf / v-raf murine sarcoma 3611 viral oncogene homolog. UCSD-Nature Molecule Pages (2010). (doi:10.1038/mp.a000307.01). 2010 [cited; Available from: http://www.signaling-gateway.org/molecule/query?afcsid=A000307

5. Baljuls A, Mueller T, Drexler HC, Hekman M, Rapp UR. Unique N-region determines low basal activity and limited inducibility of A-RAF kinase: the role of N-region in the evolutionary divergence of RAF kinase function in vertebrates. J Biol Chem 2007; 282: 26575-90.

6. Rauch J, O'Neill E, Mack B, et al. Heterogeneous Nuclear Ribonucleoprotein H Blocks MST2-Mediated Apoptosis in Cancer Cells by Regulating a-raf Transcription. Cancer Res 2010; 70: 1679-88.

7. Downward J. Targeting RAS signalling pathways in cancer therapy. Nat Rev Cancer 2003; 3: 11-22.

8. Karnoub AE, Weinberg RA. Ras oncogenes: split personalities. Nat Rev Mol Cell Biol 2008; 9: 517-31.

9. Pratilas CA, Solit DB. Targeting the mitogen-activated protein kinase pathway: physiological feedback and drug response. Clin Cancer Res 2010; 16: 3329-34.

10. Niault TS, Baccarini M. Targets of Raf in tumorigenesis. Carcinogenesis 2010; 31: 1165-74.

11. Zebisch A, Troppmair J. Back to the roots: the remarkable RAF oncogene story. Cell Mol Life Sci 2006; 63: 1314-30.

12. Hagemann C, Gloger J, Anacker J, et al. RAF expression in human astrocytic tumors. Int J Mol Med 2009; 23: 17-31.

13. Kisanuki H, Choi YL, Wada T, et al. Retroviral expression screening of oncogenes in pancreatic ductal carcinoma. Eur J Cancer 2005; 41: 2170-5.

14. Mark GE, Seeley TW, Shows TB, Mountz JD. Pks, a raf-related sequence in humans. Proc Natl Acad Sci U S A 1986; 83: 6312-6.

15. Rauch J, Ahlemann M, Schaffrik M, et al. Allogenic antibody-mediated identification of head and neck cancer antigens. Biochem Biophys Res Commun 2004; 323: 156-62.

16. Papin C, Denouel-Galy A, Laugier D, Calothy G, Eychene A. Modulation of kinase activity and oncogenic properties by alternative splicing reveals a novel regulatory mechanism for B-Raf. J Biol Chem 1998; 273: 24939-47.

17. Papin C, Eychene A, Brunet A, et al. B-Raf protein isoforms interact with and phosphorylate Mek-1 on serine residues 218 and 222. Oncogene 1995; 10: 1647-51.

18. Baitei EY, Zou M, Al-Mohanna F, et al. Aberrant BRAF splicing as an alternative mechanism for oncogenic B-Raf activation in thyroid carcinoma. J Pathol 2009; 217: 707-15.

19. He C, Zhou F, Zuo Z, Cheng H, Zhou R. A global view of cancer-specific transcript variants by subtractive transcriptome-wide analysis. PLoS One 2009; 4: e4732.

20. Yokoyama T, Takano K, Yoshida A, et al. DA-Raf1, a competent intrinsic dominant-negative antagonist of the Ras-ERK pathway, is required for myogenic differentiation. J Cell Biol 2007; 177: 781-93.

21. Nekhoroshkova E, Albert S, Becker M, Rapp UR. A-RAF Kinase Functions in ARF6 Regulated Endocytic Membrane Traffic. PLoS ONE 2009; 4: e4647.

22. Pelengaris S, Khan M, Evan G. c-MYC: more than just a matter of life and death. Nat Rev Cancer 2002; 2: 764-76.

23. Adhikary S, Eilers M. Transcriptional regulation and transformation by Myc proteins. Nat Rev Mol Cell Biol 2005; 6: 635-45.

24. Zeller KI, Jegga AG, Aronow BJ, O'Donnell KA, Dang CV. An integrated database of genes responsive to the Myc oncogenic transcription factor: identification of direct genomic targets. Genome Biol 2003; 4: R69.

25. Zeller KI, Zhao X, Lee CW, et al. Global mapping of c-Myc binding sites and target gene networks in human B cells. Proc Natl Acad Sci U S A 2006; 103: 17834-9.

26. Dang CV, O'Donnell KA, Zeller KI, Nguyen T, Osthus RC, Li F. The c-Myc target gene network. Semin Cancer Biol 2006; 16: 253-64.

27. Mayer A, Andratschke M, Pauli C, Graefe H, Kristina K, Wollenberg B. Generation of an autologous cell system for immunotherapy of squamous cell carcinoma of the head and neck. Anticancer Res 2005; 25: 4075-80.

28. Matallanas D, Sanz-Moreno V, Arozarena I, et al. Distinct utilization of effectors and biological outcomes resulting from site-specific Ras activation: Ras functions in lipid rafts and Golgi complex are dispensable for proliferation and transformation. Mol Cell Biol 2006; 26: 100-16.

29. O'Neill E, Rushworth L, Baccarini M, Kolch W. Role of the kinase MST2 in suppression of apoptosis by the proto-oncogene product Raf-1. Science 2004; 306: 2267-70.

30. Karolchik D, Baertsch R, Diekhans M, et al. The UCSC Genome Browser Database. Nucleic Acids Res 2003; 31: 51-4.

31. Birney E, Stamatoyannopoulos JA, Dutta A, et al. Identification and analysis of functional elements in 1% of the human genome by the ENCODE pilot project. Nature 2007; 447: 799-816.

32. Weischenfeldt J, Lykke-Andersen J, Porse B. Messenger RNA surveillance: neutralizing natural nonsense. Curr Biol 2005; 15: R559-62.

33. Kolch W, Heidecker G, Lloyd P, Rapp UR. Raf-1 protein kinase is required for growth of induced NIH/3T3 cells. Nature 1991; 349: 426-8.

34. Schubbert S, Shannon K, Bollag G. Hyperactive Ras in developmental disorders and cancer. Nat Rev Cancer 2007; 7: 295-308.

35. Littlewood TD, Hancock DC, Danielian PS, Parker MG, Evan GI. A modified oestrogen receptor ligand-binding domain as an improved switch for the regulation of heterologous proteins. Nucleic Acids Res 1995; 23: 1686-90.

36. Wang ET, Sandberg R, Luo S, et al. Alternative isoform regulation in human tissue transcriptomes. Nature 2008; 456: 470-6.

37. Garcia-Blanco MA, Baraniak AP, Lasda EL. Alternative splicing in disease and therapy. Nat Biotechnol 2004; 22: 535-46.

38. Wang GS, Cooper TA. Splicing in disease: disruption of the splicing code and the decoding machinery. Nat Rev Genet 2007; 8: 749-61.

39. Venables JP. Aberrant and alternative splicing in cancer. Cancer Res 2004; 64: 7647-54.

40. Venables JP. Unbalanced alternative splicing and its significance in cancer. Bioessays 2006; 28: 378-86.

41. Carpenter B, MacKay C, Alnabulsi A, et al. The roles of heterogeneous nuclear ribonucleoproteins in tumour development and progression. Biochim Biophys Acta 2006; 1765: 85-100.

42. Garneau D, Revil T, Fisette JF, Chabot B. Heterogeneous nuclear ribonucleoprotein F/H proteins modulate the alternative splicing of the apoptotic mediator Bcl-x. J Biol Chem 2005; 280: 22641-50.

43. Rooke N, Markovtsov V, Cagavi E, Black DL. Roles for SR proteins and hnRNP A1 in the regulation of c-src exon N1. Mol Cell Biol 2003; 23: 1874-84.

44. Markovtsov V, Nikolic JM, Goldman JA, Turck CW, Chou MY, Black DL. Cooperative assembly of an hnRNP complex induced by a tissue-specific homolog of polypyrimidine tract binding protein. Mol Cell Biol 2000; 20: 7463-79.

45. Pan Q, Saltzman AL, Kim YK, et al. Quantitative microarray profiling provides evidence against widespread coupling of alternative splicing with nonsense-mediated mRNA decay to control gene expression. Genes Dev 2006; 20: 153-8.

46. Kolch W, Philipp A, Mischak H, et al. Inhibition of Raf-1 signaling by a monoclonal antibody, which interferes with Raf-1 activation and with Mek substrate binding. Oncogene 1996; 13: 1305-14.

47. David CJ, Chen M, Assanah M, Canoll P, Manley JL. HnRNP proteins controlled by c-Myc deregulate pyruvate kinase mRNA splicing in cancer. Nature 2009; 463: 364-8.

48. Mazurek S, Boschek CB, Hugo F, Eigenbrodt E. Pyruvate kinase type M2 and its role in tumor growth and spreading. Semin Cancer Biol 2005; 15: 300-8.

49. Mazurek S, Drexler HC, Troppmair J, Eigenbrodt E, Rapp UR. Regulation of pyruvate kinase type M2 by A-Raf: a possible glycolytic stop or go mechanism. Anticancer Res 2007; 27: 3963-71.

Figure legends

Figure 1: The A-Raf$_{short}$ isoform expression is induced after hnRNP H knock-down. (A) *a-raf$_{short}$, a-raf$_{WT/short}$,* and *hnRNP H* mRNA expression in HeLa cells was analyzed by RT-PCR after transfection with control or hnRNP H-specific siRNA (siRNA#1). Shown is a representative result from two independent experiments. **(B)** A-Raf$_{short}$, A-Raf$_{WT}$, and hnRNP H protein expression was analysed by immunoblotting after transfection with control or hnRNP H-specific siRNA (siRNA#1). As a positive control for A-Raf$_{short}$, a lysate containing transfected recombinant HA-tagged A-Raf$_{short}$ was used. Shown are the representative results from two independent experiments. **(C) Pre-adsorption of polyclonal A-Raf antibodies with peptides used for immunisation abrogated binding of A-Raf but not HA-specific antibody.** Increasing concentrations of HA-tagged A-Raf$_{short}$ was expressed in HeLa and analysed by immunoblotting using HA- or A-Raf N-terminus specific antibodies. The A-Raf N-terminus specific antibody but not the HA-antibody signal was blocked by adding the A-Raf N-terminal peptide as competitor, showing that the detection of the A-Raf$_{short}$ isoform to be specific. Shown are the representative results from two independent experiments.

Figure 2: The A-Raf$_{short}$ protein does not interact with MST2. (A) Flag-tagged MST2 together with HA-tagged A-Raf$_{wt}$ or A-Raf$_{short}$, respectively, were expressed in HeLa cells. MST2 and A-Raf isoforms were immunoprecipitated (IP) using flag-tag specific antibodies. Flag-MST2 and A-Raf$_{wt}$, but not the short isoform A-Raf$_{short}$, co-precipitated as shown by immunoblotting (WB). Shown are the representative results from three independent experiments. **(B)** HA-tagged A-Raf$_{wt}$ or A-Raf$_{short}$ were expressed in HeLa cells. Endogenous MST2 and the HA-tagged A-Raf isoforms were immunoprecipitated (IP) with HA-tag or MST2 specific antibodies. MST2 and A-Raf$_{wt}$, but not A-Raf$_{short}$, co-precipitated. Shown are the representative results from three independent experiments. **(C) A-Raf$_{wt}$ but not A-Raf$_{short}$ can suppress MST2 kinase activity.** HeLa cells were transfected with hnRNP H (siRNA#1) and control siRNA. Where indicated, HA-A-Raf$_{wt}$, HA-A-Raf$_{short}$, or control expression plasmids were co-transfected. MST2 kinase activity was assessed by in-gel kinase assays. **(D) A-Raf$_{wt}$ but not A-Raf$_{short}$ can suppress apoptosis induced by hnRNP H depletion.** Apoptosis was determined in HeLa cells following transfection with hnRNP H-siRNA. Where indicated, cells were co-transfected with A-Raf$_{wt}$, A-Raf$_{short}$ expression plasmids. The data represent mean percentage of apoptosis with SD of three experiments. Additionally, cells were lysed, and expression of flag-tagged A-Raf, Caspase-3, and PARP was assessed by immunoblotting (lower panels).

Figure 3: A-Raf$_{short}$ inhibits Ras-ERK signalling. (A) Numbers of HeLa, GHD-1, and HCT-116 cells were determined in a time kinetic following overexpresion of A-Raf$_{short}$ or A-Raf$_{WT}$. Results represent the mean with standard deviation (SD) of three independent experiments. **(B) A-Raf$_{short}$ inhibits phosphorylation of ERK.** Hela

cells were transfected with increasing amounts of A-Raf$_{short}$ or A-Raf$_{WT}$. Cells were serum-starved for 16 hours (0.1% FCS) or serum-stimulated (10% FCS) for 5min after starvation as indicated. Lysates were immunoblotted for expression of the transfected flag-tagged Raf isoforms, phopho-ERK1/2, and ERK1/2 as loading control. **(C) A-Raf$_{short}$ inhibits ERK phosphorylation without affecting AKT phosphorylation.** Hela cells were transfected with either A-Raf$_{short}$ or A-Raf$_{WT}$. Cells were serum-starved for 16 hours (0.1% FCS) or serum-stimulated (10% FCS) for 5min after starvation as indicated. Lysates were immunoblotted for expression of the transfected flag-tagged Raf isoforms, phopho-ERK1/2, ERK1/2, phospho-AKT, and AKT. **(D) A-Raf$_{short}$ siRNA#3 specifically downregulates the A-Raf$_{short}$ isoform and increases ERK phosphorylation.** (left panel) Hela cells were transfected with four different siRNAs for A-Raf$_{short}$ or A-Raf$_{WT}$. Cells were serum-starved for 16 hours and serum-stimulated for 5min. Lysates were immunoblotted for expression of A-Raf$_{short}$, A-Raf$_{WT}$, phopho-ERK1/2, and ERK1/2. Shown are the representative results from two independent experiments. (right panel) Hela cells were transfected with either A-Raf$_{short}$ siRNA#3 or control siRNA. Cells were serum-starved for 16 hours (0.1% FCS) or serum-stimulated (10% FCS) for 5min after starvation as indicated. Lysates were immunoblotted for expression of A-Raf$_{short}$, phopho-ERK1/2, and ERK1/2.

Figure 4: A-Raf$_{short}$ interacts with activated Ras inhibiting Ras-ERK signalling. **(A)** Flag-tagged A-Raf$_{short}$ or A-Raf$_{WT}$ were transfected in HeLa cells. Cells were serum-starved for 16 hours (0.1% FCS) or serum-stimulated (10% FCS) for 5min after starvation as indicated. A-Raf isoforms were immunoprecipitated with flag-tag specific antibodies, and analysed by immunoblotting for the interaction with Ras. **(B)** En-

dogenous Ras was immunoprecipitated from lysates of HeLa cells, which had been serum starved (0.1% FCS, 16 hours) or treated with full medium (10% FCS) after serum-starvation using a specifc antibody for Ras, and analysed by immunoblotting (upper panel). As an isotype control, an antibody specific for GFP was used (middle panel, 'Isotype'). Lysates were immunoblotted for expression of A-Raf$_{short}$, Ras, B-Raf, phosphorylated ERK1/2, and ERK1/2 as loading control (lower panel). LC - light chain immunoglobulin. Shown are the representative results from three independent experiments. **(C) A-Raf$_{short}$ binds better to Ras.** Either fixed or increasing amounts of Flag-tagged A-Raf$_{short}$ or A-Raf$_{WT}$ togther with HA-tagged H-Ras-V12 were transfected in HeLa cells as indicated. Cells were serum-starved for 16 hours (0.1% FCS) and serum-stimulated (10% FCS) for 5min after starvation. Ras complexes were immunoprecipitated, and analysed by immunoblotting for the A-Raf isoform interaction. **(D) A-Raf$_{short}$ inhibits Ras-induced cellular tranformation.** NIH3T3 fibroblasts were tranfected with hyperactive Ras constructs. Cells were co-tranfected with either A-Raf$_{WT}$ or A-Raf$_{short}$ as indicated (left panel). Numbers indicate average number of foci per microgram of DNA (Ras constructs) (right panel). Error bars represent standard deviation of at least three independent experiments.

Figure 5: c-Myc regulates hnRNP H expression. (A) Hela cells were transfected with either c-myc siRNA or control siRNA. Lysates were immunoblotted for expression of c-Myc, hnRNP H, A-Raf$_{WT}$ or A-Raf$_{short}$, and ERK1/2 using specific antibodies. **(B)** HeLa cells were transfected with the 4-hydroxytamoxifen (4-OHT)-inducible chimeric MycER^{T}, hnRNP H siRNA, or Control siRNA as indicated. Following transfection, cells were serum-starved for 16 hours (0.1% FCS) and MycER^{T} induced with 4-OHT (100nM). 0, 4, and 8 hours post induction, cells were lysed and lysates im-

munoblotted for expression of the hnRNP H, A-Raf$_{WT}$ or A-Raf$_{short}$, and ERK1/2 as loading control. **(C)** HeLa cells were serum-starved for 18 hours (0.1% FCS) and stimulated with EGF (10nM) as indicated. 5, 30, 60, 180, and 360min post stimulation, cells were lysed and lysates immunoblotted for expression of the c-Myc, hnRNP H, A-Raf$_{WT}$, A-Raf$_{short}$, phopho-ERK1/2, and ERK1/2 as loading control. **(D) c-Myc binds to promotor elements of the human HNRNPH1 genomic locus**. c-Myc Chromatin IPs in either serum-starved (18hrs, 0.1% FCS) or EGF-stimulated Hela cells were analyzed using semi-quantitative Real-time PCR. PCR primer pairs correspond to elements in the human hnRNP H promotor region as depicted. The red line indicates no change in c-Myc-specific enrichment. Shown are the representative results from three independent experiments, error bars represent standard deviations.

Figure 6: Expression of *c-myc, hnRNP H,* and *a-raf* isoforms in carcinomas and adjacent normal tissues. (A) The expression of *a-raf$_{short}$*, *a-raf$_{WT}$*, *hnRNP H,* and *c-myc* mRNA was assessed in head and neck (HNSCC) tumours (T) and normal adjacent tissues (N) by semi-quantitative RT-PCR. *Mapk1* mRNA levels were determined as a loading control. **(B)** Relative expression of *c-myc*, *hnRNP H* and *a-raf* isoforms in head and neck tissues (left panel) and in colon carcinomas (n=29) and adjacent normal tissues (n=29) (right panel) according to disease state. Shown are boxplots where boxes indicate the median (line) and IQR, whiskers show the range, and asterisks indicate outliers. **(C)** Scatterplots are used to illustrate the degree of correlation between *c-myc/hnRNPH*, *hnRNP H/a-raf$_{WT}$*, and *hnRNPH*/*a-raf$_{short}$* relative expression in tumours (red) and normal tissues (blue). **(D) Hypothesis and model for hnRNP H-mediated A-Raf isoform selection.** In normal cells, low levels of the proto-oncogene c-Myc and the splice factor hnRNP H ensure increased A-Raf$_{short}$ levels

thus keeping proliferation via MAPK signalling in check. Tumour cells show higher expression of both c-Myc and hnRNP H thereby enabling sufficient A-Raf$_{WT}$ expression and keeping MST-2 mediated apoptosis in check. Additionally, A-Raf$_{short}$ is downregulated in tumour cells enabling increased proliferation.

Figure 1
(Rauch *et al.*)

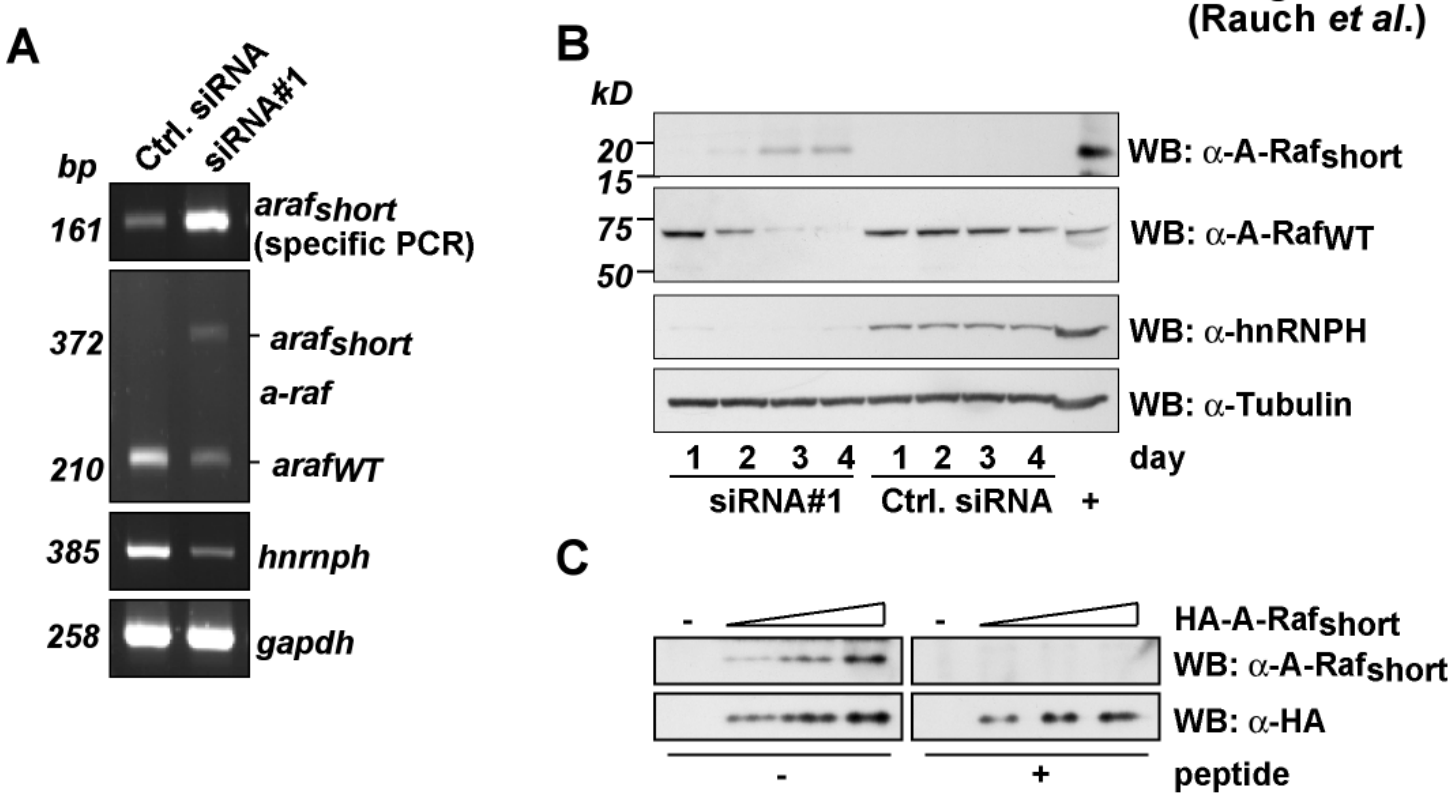

Figure 2 (Rauch *et al.*)

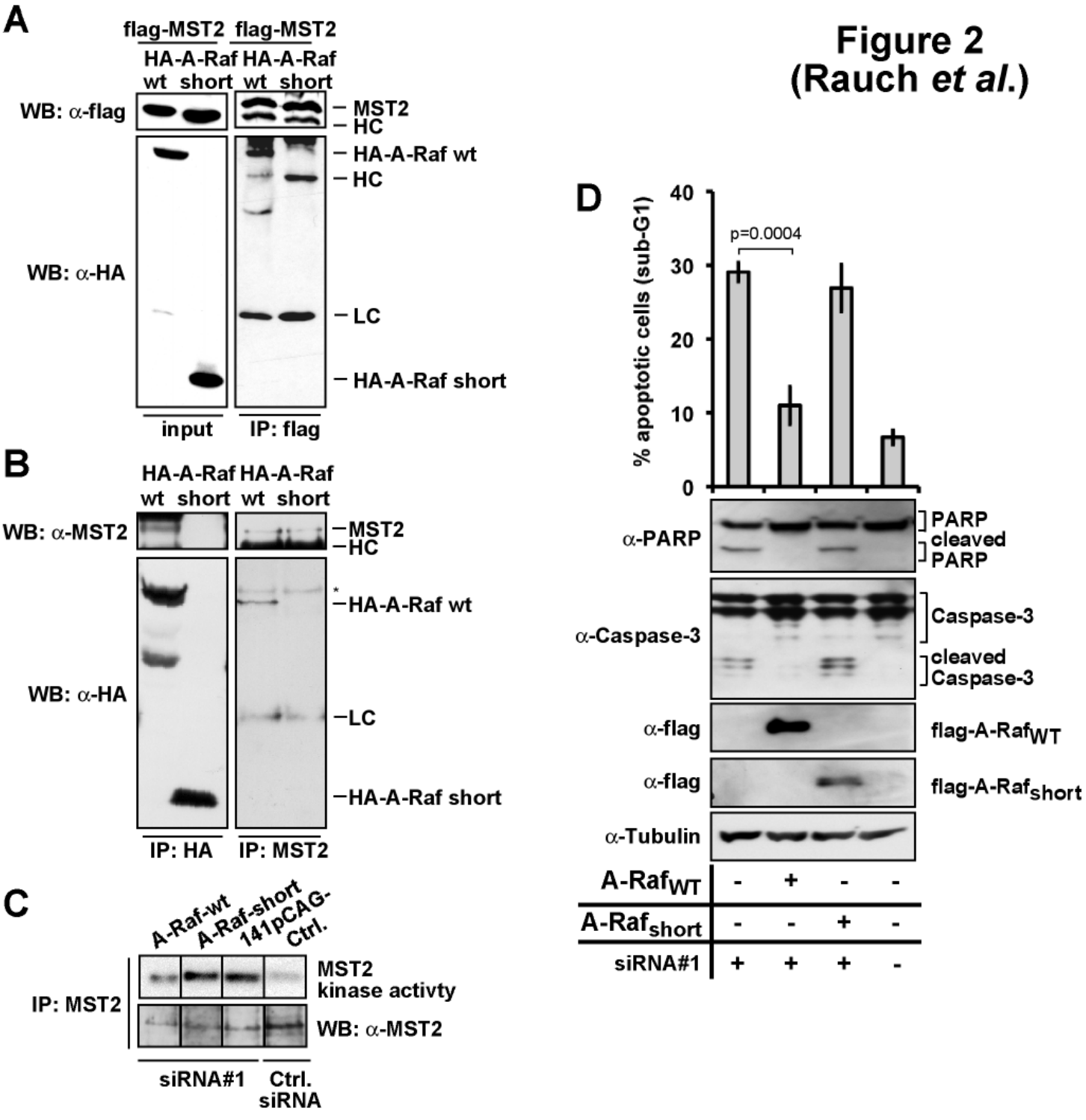

Figure 3
(Rauch *et al.*)

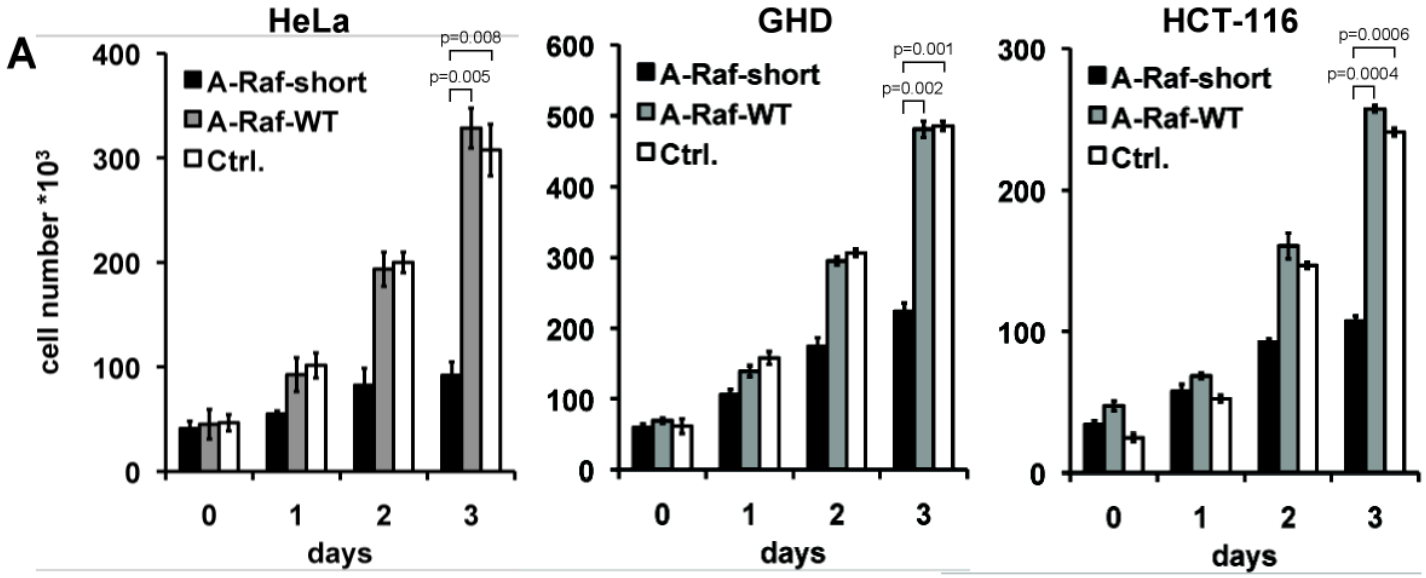

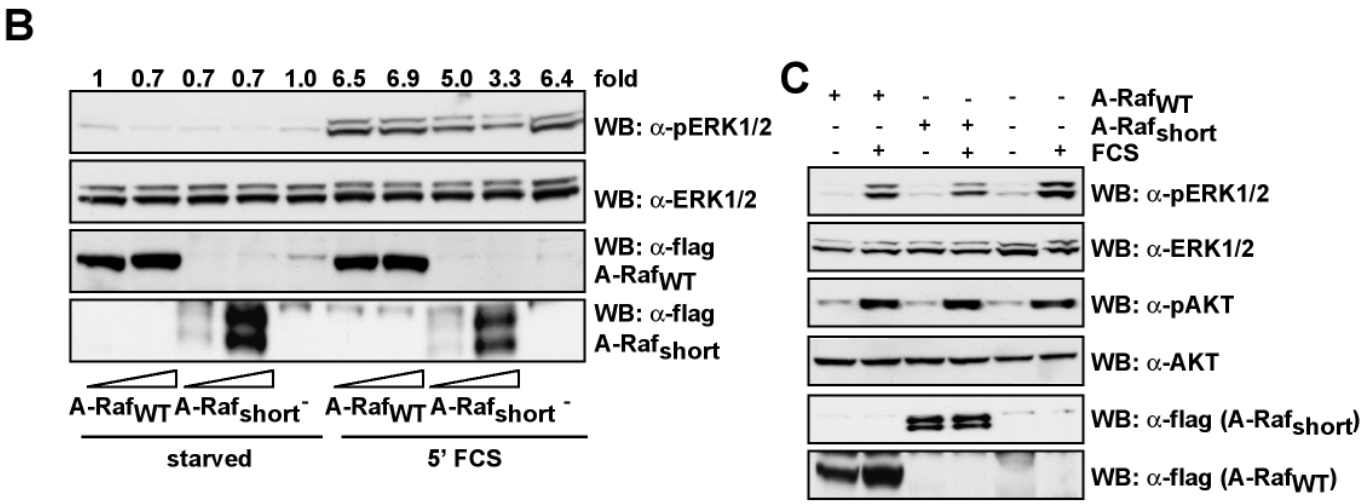

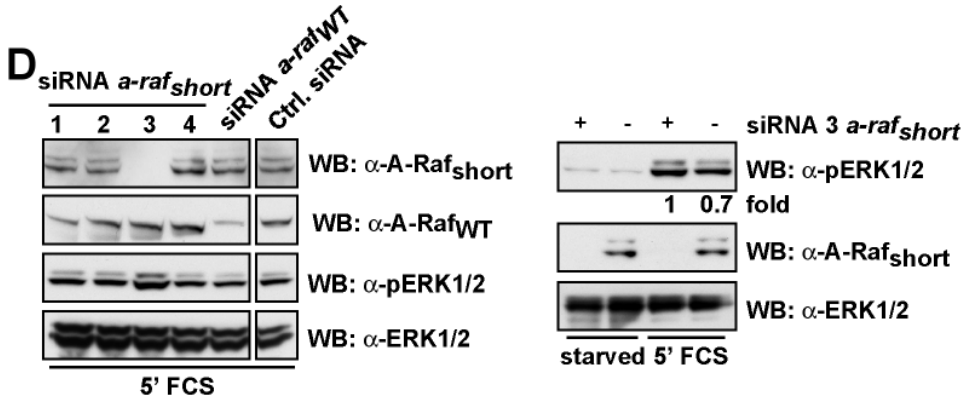

Figure 4
(Rauch *et al.*)

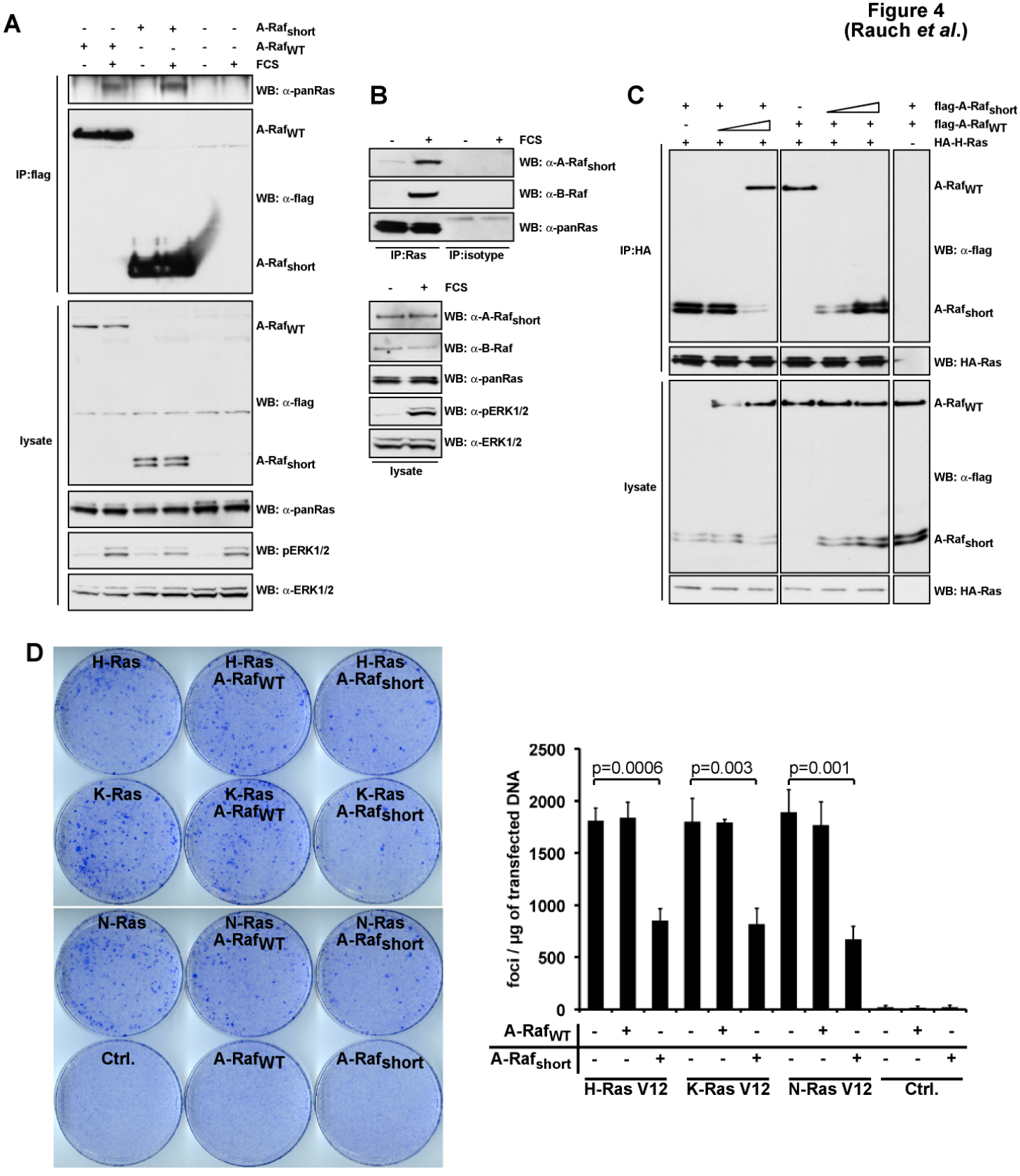

Figure 5
(Rauch *et al.*)

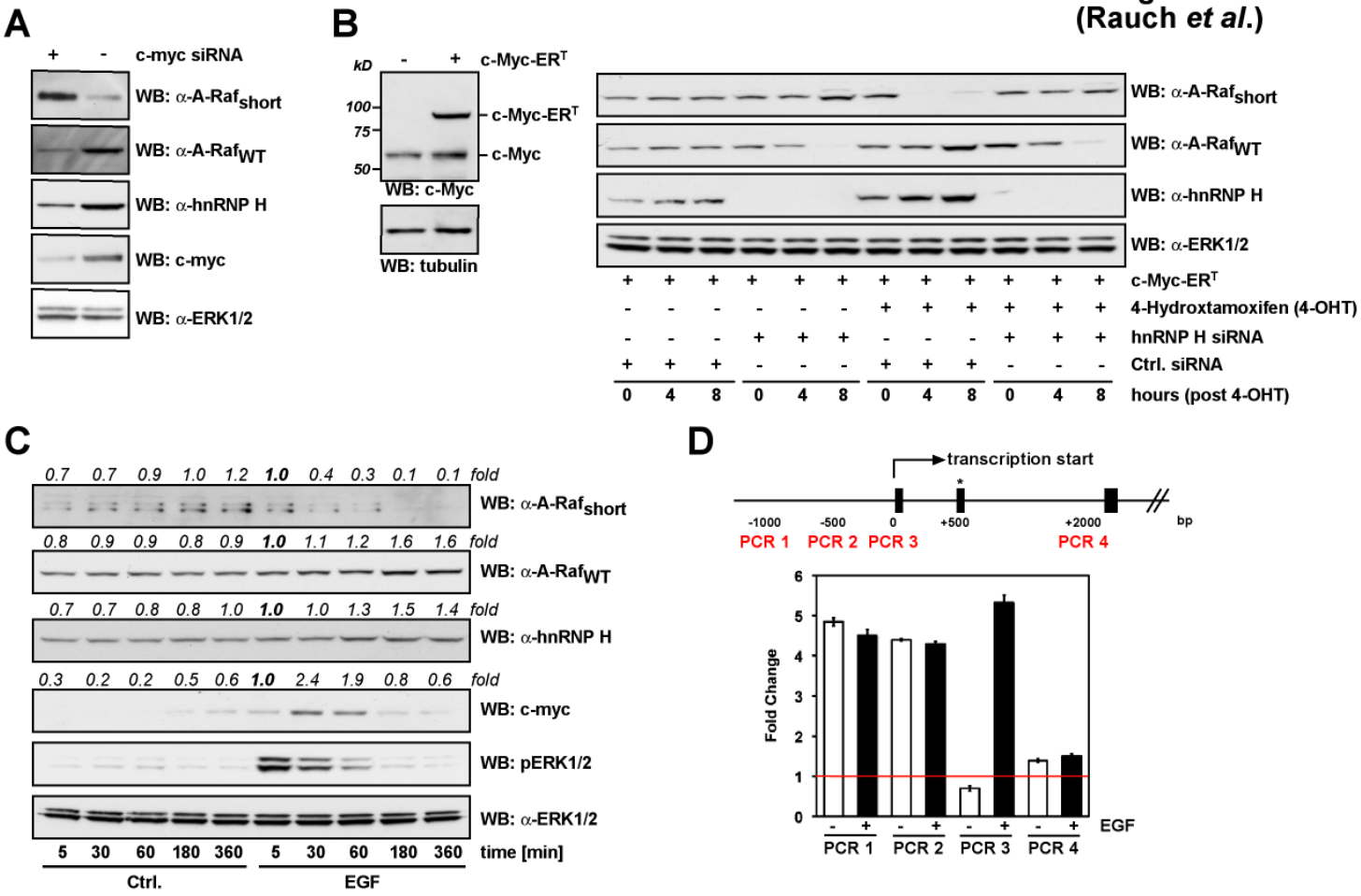

Figure 6
(Rauch *et al.*)

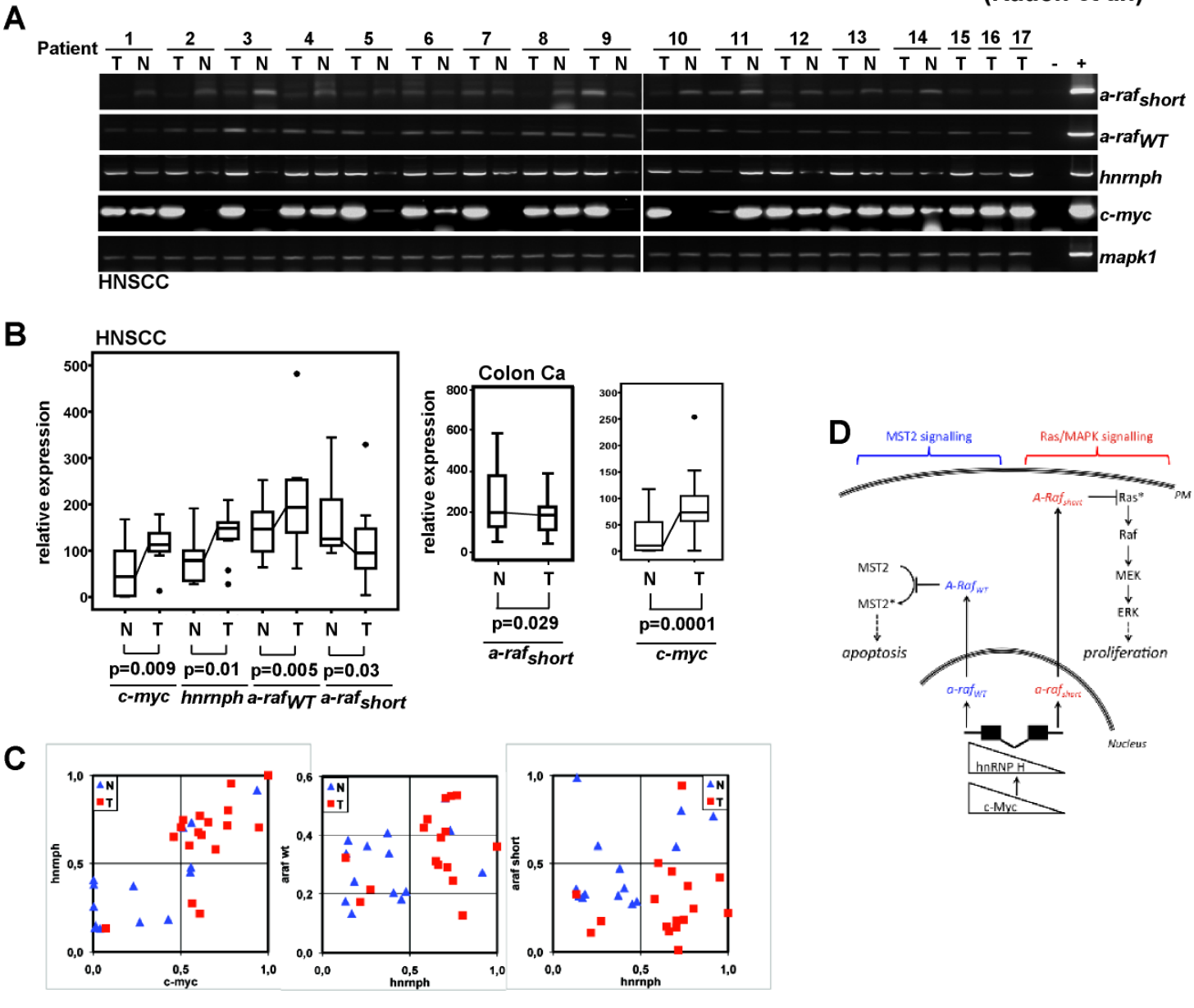

Supplementary Figure Lgends:

Supplementary Figure S1: (A) Nucleotide sequence of exons (red) and introns (blue) retained in the human *a-raf*$_{short}$ mRNA and corresponding amino acid sequence. Asterisks in intron 1 and 3 indicate splicing. Shaded areas represent amino acid sequences lacking in the generic A-Raf protein. Red boxes indicate G-rich regions. PTS; pre-terminal stop-codon. **(B)** Alignment of all four known human A-Raf isoforms. Shown are protein sequences where red letters indicate amino acids derived from intronic sequences which are exclusively found in the A-Raf$_{short}$ isoform.

Supplementary Figure S2: Schematic overview of *a-raf* isoforms. (A) Shown are the exon/intron structures of mRNAs and corresponding proteins of the so far known different *a-raf* isoforms. Boxes indicate exons, lines indcate introns. E: exon; i: intron; UTR: untranslated region. **(B)** Functional domains of *a-raf* isoforms. The numbers indicate amino acid residues of human A-Raf. CR: conserved region; RBD: Ras binding domain; CRD: Cysteine rich domain; S/T Rich: Serine/Threonine rich domain

Supplementary Figure S3: A-Raf$_{short}$ acts upstream of Raf. (A) NIH3T3 fibroblasts were tranfected with an oncogenic viral Raf (vRaf) construct (1µg). Cells were co-tranfected with A-Raf$_{short}$ as indicated (1µg). After two weeks in culture foci were stained with GIEMSA and scored. **(B)** Numbers indicate average number of foci per microgram of DNA (vRaf construct). Error bars represent standard deviation of at least three independent experiments. n.s.; not significant. **A-Raf$_{short}$, like daRaf1 and daRaf2, inhibits Ras-induced cellular tranformation. (C)** NIH3T3 fibroblasts were tranfected with hyperactive Ras constructs (100ng). Cells were co-tranfected with either A-Raf$_{short}$, daRaf1, or daRaf2 as indicated (1µg).

After two weeks in culture foci were stained with GIEMSA and scored. **(D)** Numbers indicate average number of foci per microgram of DNA (Ras constructs). Error bars represent standard deviation of at least three independent experiments. * $p \leq 0.05$. ** $p \leq 0.01$.

Supplementary Figure S4: The A-Raf$_{short}$ isoform expression is induced by cell density. (A) HeLa cells were grown to medium conluency (< 60%) or full confluency (>90%) and grown in DMEM supplemented with increasing concentrations of FCS as indicated. Lysates were immunoblotted for expression of A-Raf$_{short}$, and tubulin as loading control. Shown are the representative results from three independent experiments. **(B)** HeLa cells were grown to increasing condluency (left panel) and lysates were immunoblotted for expression of A-Raf$_{short}$, A-Raf$_{WT}$, c-Myc, hnRNPH, pERK1/2 and ERK1/2 as loading control (right panel). Shown are the representative results from three independent experiments. The protein expression levels of A-Raf$_{wt}$ and A-Raf$_{short}$ were quantified using ImageJ (upper right). All values were standardized using ERK1/2. Shown are relative ODs. **(C) hnNRP H is not regulated by the MAPK pathway.** Hela cells were treated with the ERK1/2 inhibitor UO 126 for a timecourse of 12 hours as indicated. Lysates were immunoblotted for expression of A-Raf$_{short}$, hnRNPH, pERK1/2 and ERK1/2 as loading control.

Supplementary Figure S5: Human HNRNPH1 genomic locus and binding of c-Myc. (A) DNA sequences and annotation data for c-Myc binding (human genome assembly Mar. 2006, NCBI36/hg18) were retrieved from the Genome Browsers of the University of California Santa Cruz (1). We analyzed the genomic locus of the human HNRNPH1 gene (coordinates: chr5:178,971,093-178,987,247) and used the c-Myc ChIP annotation provided in UCSC table 'ENCODE Open Chromatin, Duke/UNC/UT' showing density graphs for the following cell

lines (2): GM12878 (lymphoblastoid cell line), H1-hESC (Human Embryonic Stem Cells), HeLa-S3 (cervical carcinoma cell line), HepG2 (liver carcinoma cell line), HUVEC (Human Umbilical Vein Endothelial Cell line), K562 (leukemia cell line). ChIP-seq results are shown as number of DNA fragments obtained at each position relative to the genomic average. **(B)** Positions of the PCR amplicons used for c-Myc ChIP analysis.

Supplementary Figure S6: Protein expression of A-Raf$_{wt}$, and A-Raf$_{short}$ in HNSCC and normal adjacent tissues. (A) The expression of protein was assessed by immunoblotting in normal mucosa (n=3) and carcinoma tissues (n=3) of the head and neck area. ERK1/2 levels were determined as a loading control. **(B)** Relative quantified expression of A-Raf isoforms. Shown are dotplots where asterisks and dots indicate the median and individual (respectively), relative expressions levels.

Supplemental Experimental Procedures

siRNA sequences

The following siRNA sequences were used:

hnRNPH: 5'-GGAGCUGGCUUUGAGAGGA dTdT-3'
A-Raf$_{WT}$: Silencer Validated siRNA 151 (Ambion, Austin, US)
A-Raf$_{short}$ (1): 5'-AAUGGCAGGGGCUGUGGAUGGdTdT-3'
A-Raf$_{short}$ (2): 5'-AACUCUGGGAUCAAAAGGGUGdTdT-3'
A-Raf$_{short}$ (3): 5'-AAUCAGGACUGCUGUGUGGUCdTdT-3'
A-Raf$_{short}$ (4): 5'-AUGUUGGGGGUGUCCUUGACdTdT-3'
c-Myc: ON-TARGETplus SMARTpool Human MYC (Dharmacon)

Semi-quantitative PCR

Cell lines and human tissues were analysed by semi-quantitative PCR for the expression of the following human mRNAs *c-myc*, *hnrnph*, *a-raf$_{WT/short}$, a-raf$_{WT}$, a-raf$_{short}$, daraf1, daraf2, beta-actin, gapdh, and mapk.* PCR conditions were denaturing at 95 °C for 30 seconds, annealing for 30 seconds, extension at 72 °C for 30 seconds).

The following primers were used; the amplicon size of the PCR product given in brackets:

hnRNPH (385bp):	5'-AAAATGGGGCTCAAGGTATTCG-3' 5'-GCTATTTCCTGTGAAGCAAACTGC-3'
a-raf$_{WT/short}$: (*a-raf$_{short}$* 372bp; *a-raf$_{WT}$* 210bp):	5'-ATGGAGCCACCACGGGGC-3' 5'-CGTCTTTCGTCCCTTGATGAGTC-3'
a-raf$_{short}$ (161bp):	5'- CGGTGGTGAGTCATGGAAGC-3' 5'- GTATGTGCAGATGTAGGGGTCC-3'
hdaraf1/2: (*daraf1* 578bp, *daraf2* 695bp)	5'-CATGGAGCCACCACGGGG-3' 5'-TTCAGCTAAGGCATCCCTAC-3'
c-myc (236bp):	5'- TCCGTCCTCGGATTCTCTGC-3' 5'-CCAGTGGGCTGTGAGGAGGT-3'
gapdh (258bp):	5'-TGTCGCTCTTGAAGTCAGAGGAGA-3' 5'-AGAACATCATCCCTGCCTCTACTG-3'
mapk1 (233bp):	5'- CCTTCCAACCTGCTGCTCAACAC-3' 5'- GGAAAGATGGGCCTGTTAGAAAGC-3'
beta–actin (174bp):	5'- AGCCTCGCCTTTGCCGA-3'

5'- CTGGTGCCTGGGGCG-3'

Immunoblot analysis

Protein lysates or immunoprecipitates were resolved by SDS-PAGE (10-15%) and blotted on PVDF membrane (Millipore, Bedford, US). Protein visualisation was performed using the following antibodies in combination with HRP-conjugated secondary antibodies and the ECL system (GE-Healthcare, Munich, Germany): Polyclonal rabbit anti-human hnRNPH antibody (Bethyl Laboratories, Montgomery, US), polyclonal goat anti-human A-Raf antibody sc-408-G (Santa Cruz, Santa Cruz, US), polyclonal rabbit anti-human MST2 antibody (Stratagene, La Jolla, US), monoclonal mouse anti-human tubulin antibody sc-8035 (Santa Cruz, Santa Cruz, US), monoclonal mouse anti-human Flag antibody F3165 (Sigma, Taufkirchen, Germany), monoclonal mouse anti-HA tag antibody 3F10 (Roche Diagnostics, Mannheim, Germany), monoclonal mouse anti-human Ras antibody sc-29 (Santa Cruz, Santa Cruz, US), polyclonal rabbit anti-human B-Raf antibody sc-166 (Santa Cruz, Santa Cruz, US), monoclonal rabbit anti-human MST2 (N-term.) antibody 1943-1 (Epitomics Inc., Burliname, US), polyclonal rabbit anti-human mitogen acivated protein kinase (ERK1, ERK2) antibody M-5670 (Sigma, Taufkirchen, Germany), monoclonal mouse anti-human MAP kinase, activated (Diphosphorylated ERK-1&2) antibody M-8159 (Sigma, Taufkirchen, Germany), polyclonal rabbit anti-human caspase-3 antibody sc-7148 (Santa Cruz, Santa Cruz, US), monoclonal rabbit anti-human caspase-3 antibody (8G10) sc-9665 (Santa Cruz, Santa Cruz, US), monoclonal mouse anti-human PARP antibody (Becton Dickinson, Franklin Lakes, US), monoclonal mouse anti-human c-Myc antibody (9E10) sc-40 (Santa Cruz, Santa Cruz, US). The polyclonal anti-human antibody against endogenous A-Raf$_{short}$ was raised in rabbits using a peptide of the N-terminus of A-Raf (EPPRGPPANGAEPS) (Eurogentec Ltd, Southampton,

UK). In order to demonstrate antibody specificity, the above-mentioned peptide was added as competitor at a final concentration of 50µg peptide/µg antibody.

Chromatin Immunoprecipitation (ChIP)

HeLa cells were serum-starved for 18 hrs, stimulated with 10nM EGF for 20 min as indicated and fixed in 1% formaldehyde for 10 min. ChIP assays were performed using the SimpleChIP Enzymatic Chromatin IP Kit (Agarose Beads) (Cell Signaling, Danvers, MA) according to the manufacturer's instructions. We used the rabbit antibody against c-Myc (D84C12, Cell Signaling, Danvers, MA) and rabbit IgGs as a negative control. The purified DNA from cross-linked cells was dissolved in 50µl TE buffer; 1µl was used for PCR. As an input we used 2% chromatin before immunoprecipitation. DNA sequences were analysed by quantitative real-time PCRs (SYBR Green) in triplicate using the ABI 7900HT Sequence Detection System (Applied Biosystems, Foster City, CA) with the following thermal cycling conditions: Initial denaturation (10min, 95°C) followed by 45 cycles of denaturation (15sec, 95°C) and annealing/extension (1min, 60°C). Dissociation curves were analyzed to ensure PCR quality and to monitor primer dimers. The following primer sets were used to cover regions of the hnRNP H genomic locus as depicted in Figures 5 and S5:

PCR1: 5'-ATCTTAGGTTTTGGGCAGTGCTGC-3'
5'-TGCATCTCCCAGAGCAGAATTGGT-3'

PCR2: 5'-TAAGGGGAAGTGGAGGCACACA-3'
5'-GCGCCGCCTGTCTTCCCTTTAT-3'

PCR3: 5'-AACCCAAGCGTGTAATAATCCGCC-3'
5'-CTGCGCAACCTAAATAAGGTCCCTT-3'

PCR4: 5'-TAGCTTGGTAACACTGATCCCCTTT-3'
5'-AACATACTTCGTTGCGAGCTGTTTT-3'

Fold-change was obtained based on critical threshold (C_T) measurements calculating the signal-to-noise ratio normalized to the input. In detail, the amount of genomic DNA precipitated with specific antibody was calculated compared to the total input DNA used for each immunoprecipitation in the following way: $\Delta C_T = C_T(\text{input DNA}) - C_T(\text{specific antibody})$, where C_T are the mean threshold cycles performed in triplicates. Finally, $\Delta\Delta C_T$ was calculated using $\Delta\Delta C_T = \Delta C_T$ (c-Myc antibody) $- C_T$(IgG control antibody) and linearly transformed ($2^{\Delta\Delta CT}$) for each amplicon and sample. Error bars represent standard deviations.

Sequence and annotation data

DNA sequences and annotation data for c-Myc binding (human genome assembly Mar. 2006, NCBI36/hg18) were retrieved from the Genome Browsers of the University of California Santa Cruz (1). We analyzed the genomic locus of the human HNRNPH1 gene (coordinates: chr5: 178,971,093-178,987,247) and used the c-Myc ChIP annotation provided in UCSC table 'ENCODE Open Chromatin, Duke/UNC/UT' showing density graphs (2).

Supplemetal References

1. Karolchik D, Baertsch R, Diekhans M, et al. The UCSC Genome Browser Database. Nucleic Acids Res 2003; 31: 51-4.
2. Birney E, Stamatoyannopoulos JA, Dutta A, et al. Identification and analysis of functional elements in 1% of the human genome by the ENCODE pilot project. Nature 2007; 447: 799-816.

Suppl. Figure S1
(Rauch *et al.*)

A

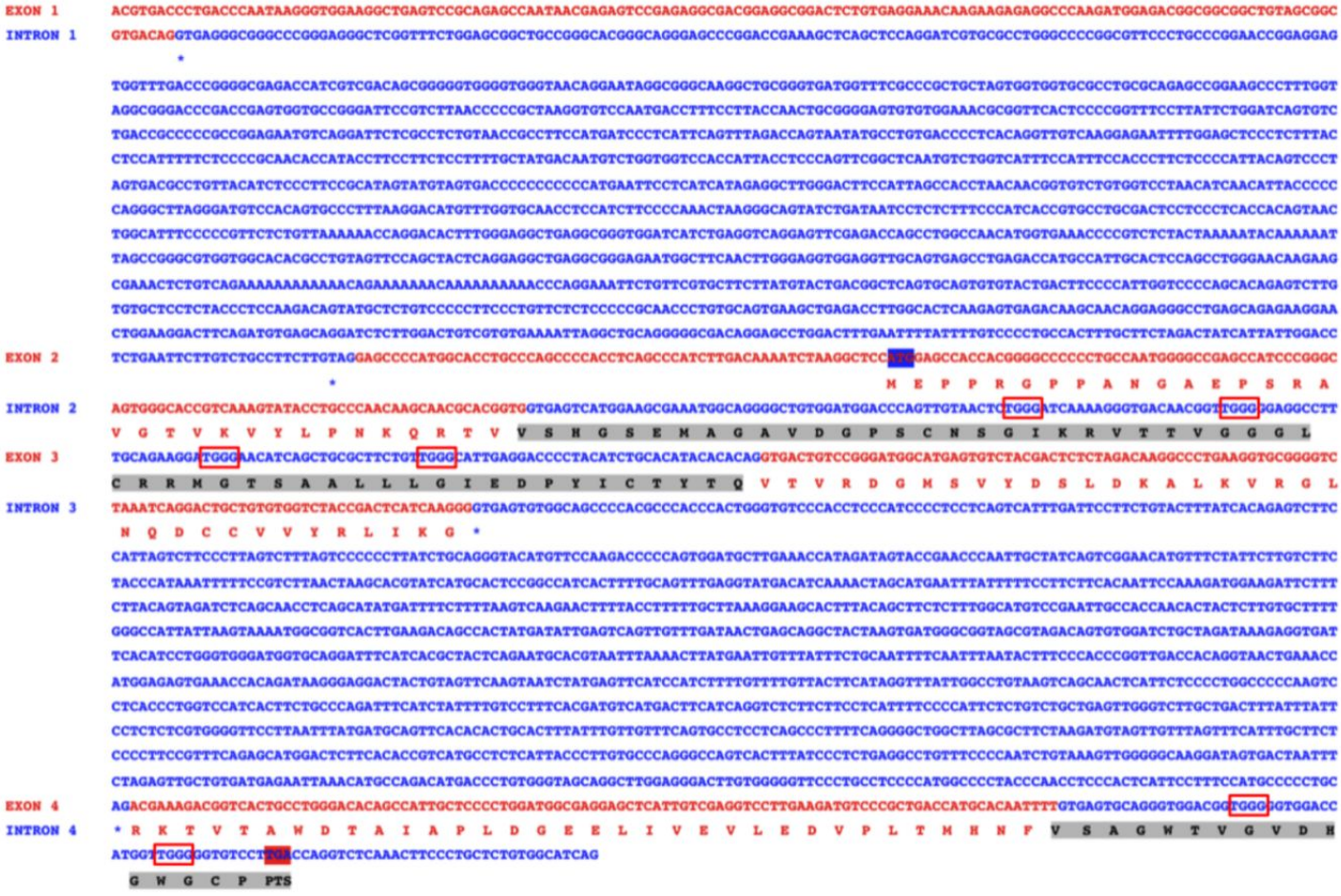

B

CLUSTAL 2.1 multiple sequence alignment

```
A-Raf-WT        MEPPRGPPANGAEPSRAVGTVKVYLPNKQRTVV----------------------------------------------------------TVRDGMSVYDSLD
A-Raf-short     MEPPRGPPANGAEPSRAVGTVKVYLPNKQRTVVSHGSEMAGAVDGPSCNSGIKRVTTVGGGLCRRMGTSAALLLGIEDPYICTYTQVTVRDGMSVYDSLD
DA-Raf1         MEPPRGPPANGAEPSRAVGTVKVYLPNKQRTVV----------------------------------------------------------TVRDGMSVYDSLD
DA-Raf2         MEPPRGPPANGAEPSRAVGTVKVYLPNKQRTVV----------------------------------------------------------TVRDGMSVYDSLD
                ********************************                                                             *************

A-Raf-WT        KALKVRGLNQDCCVVYRLIKGRKTVTAWDTAIAPLDGEELIVEVLEDVPLTMHNFVRKTFFSLAFCDFCLKFLFHGFRCQTCGYKFHQHCSSKVPTVCVD
A-Raf-short     KALKVRGLNQDCCVVYRLIKGRKTVTAWDTAIAPLDGEELIVEVLEDVPLTMHNFVSAGWTVGVDHGWGCP----------------------------
DA-Raf1         KALKVRGLNQDCCVVYRLIKGRKTVTAWDTAIAPLDGEELIVEVLEDVPLTMHNFVRKTFFSLAFCDFCLKFLFHGFRCQTCGYKFHQHCSSKVPTVCVD
DA-Raf2         KALKVRGLNQDCCVVYRLIKGRKTVTAWDTAIAPLDGEELIVEVLEDVPLTMHNFVRKTFFSLAFCDFCLKFLFHGFRCQTCGYKFHQHCSSKVPTVCVD
                ************************************************************

A-Raf-WT        MSTNRQQFYHSVQDLSGGSRQHEAPSNRPLNELLTPQGPSPRTQHCDPEHFPFPAPANAPLQRIRSTSTPNVHMVSTTAPMDSNLIQLTGQSFSTDAAGS
A-Raf-short     ------------------------------------------------------------------------------------------------------
DA-Raf1         MSTNRQQFYHSVQDLSGGSRQHEAPSNRPLNELLTPQGPR----------------------------------------------------------
DA-Raf2         MSTNRQQ-------------------------------------------------------------------------------------------------

A-Raf-WT        RGGSDGTPRGSPSPASVSSGRKSPHSKSPAEQRERKSLADDKKKVKNLGYRDSGYYWEVPPSEVQLLKRIGTGSFGTVFRGRWHGDVAVKVLKVSQPTAE
A-Raf-short     ------------------------------------------------------------------------------------------------------
DA-Raf1         ------------------------------------------------------------------------------------------------------
DA-Raf2         ------------------------------------------------------------------------------------------------------

A-Raf-WT        QAQAFKNEMQVLRKTRHVNILLFMGFMTRPGFAIITQWCEGSSLYHHLHVADTRFDMVQLIDVARQTAQGMDYLHAKNIIHRDLKSNNIFLHEGLTVKIG
A-Raf-short     ------------------------------------------------------------------------------------------------------
DA-Raf1         ------------------------------------------------------------------------------------------------------
DA-Raf2         ------------------------------------------------------------------------------------------------------

A-Raf-WT        DFGLATVKTRWSGAQPLEQPSGSVLWMAAEVIRMQDPNPYSFQSDVYAYGVVLYELMTGSLPYSHIGCRDQIIFMVGRGYLSPDLSKISSNCPKAMRRLL
A-Raf-short     ------------------------------------------------------------------------------------------------------
DA-Raf1         ------------------------------------------------------------------------------------------------------
DA-Raf2         ------------------------------------------------------------------------------------------------------

A-Raf-WT        SDCLKFQREERPLFPQILATIELLQRSLPKIERSASEPSLHRTQADELPACLLSAARLVP
A-Raf-short     ------------------------------------------------------------
DA-Raf1         ------------------------------------------------------------
DA-Raf2         ------------------------------------------------------------
```

Suppl. Figure S2 (Rauch *et al.*)

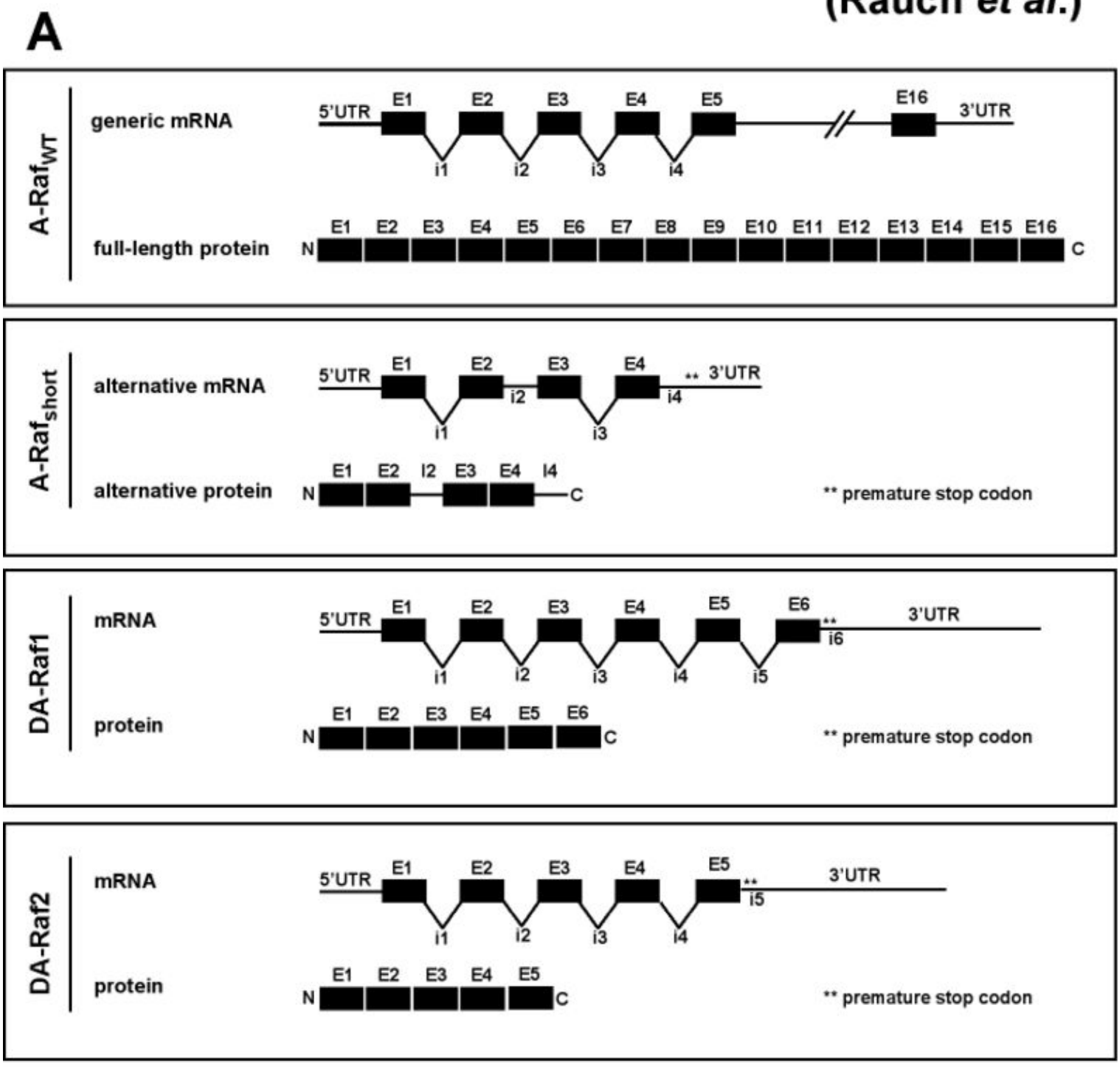

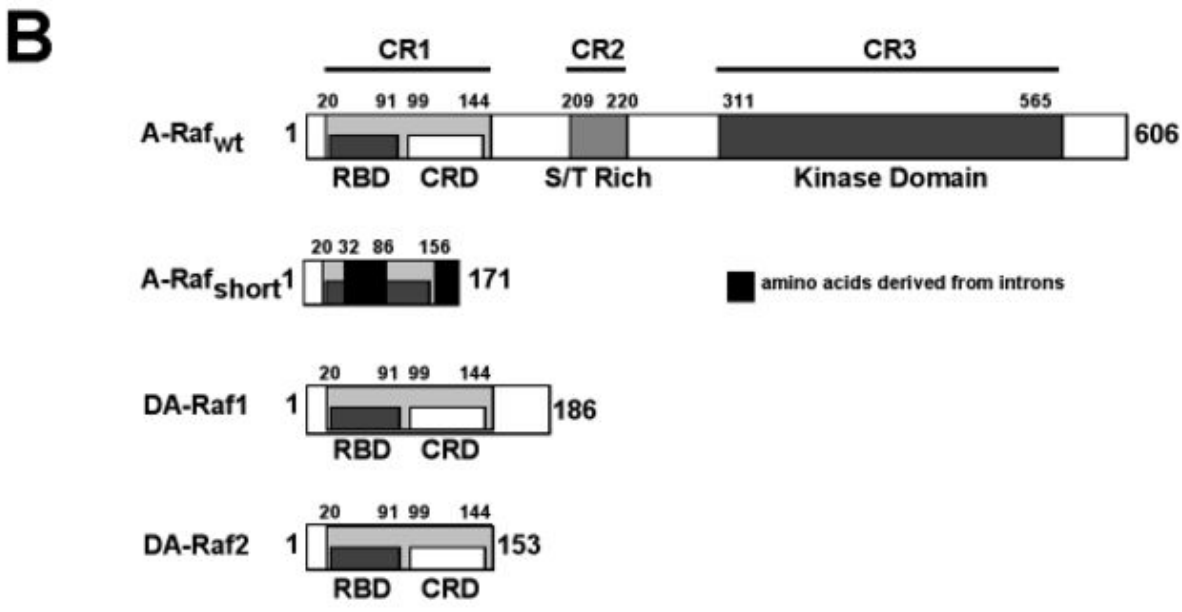

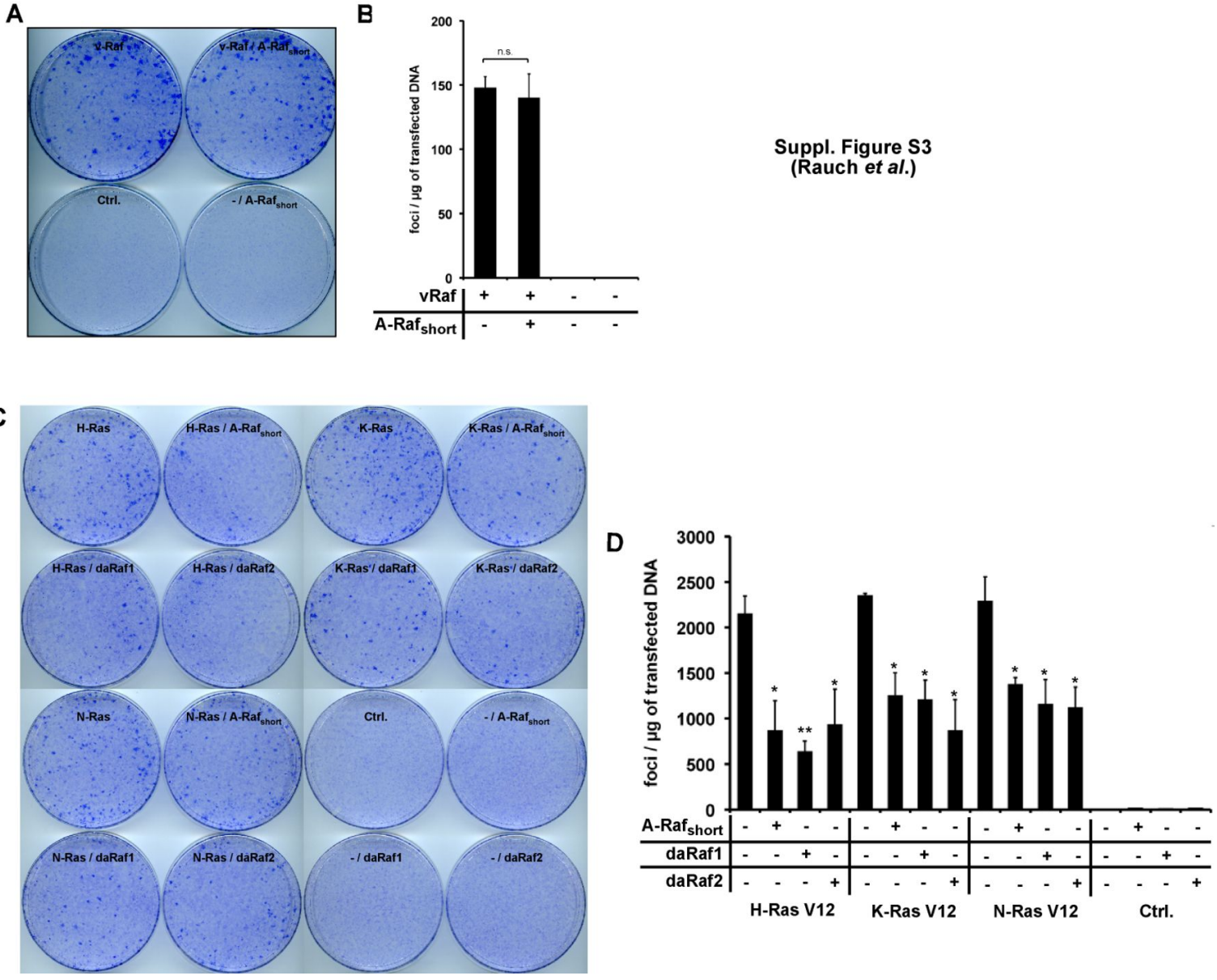

Suppl. Figure S3
(Rauch *et al.*)

Suppl. Figure S4
(Rauch *et al.*)

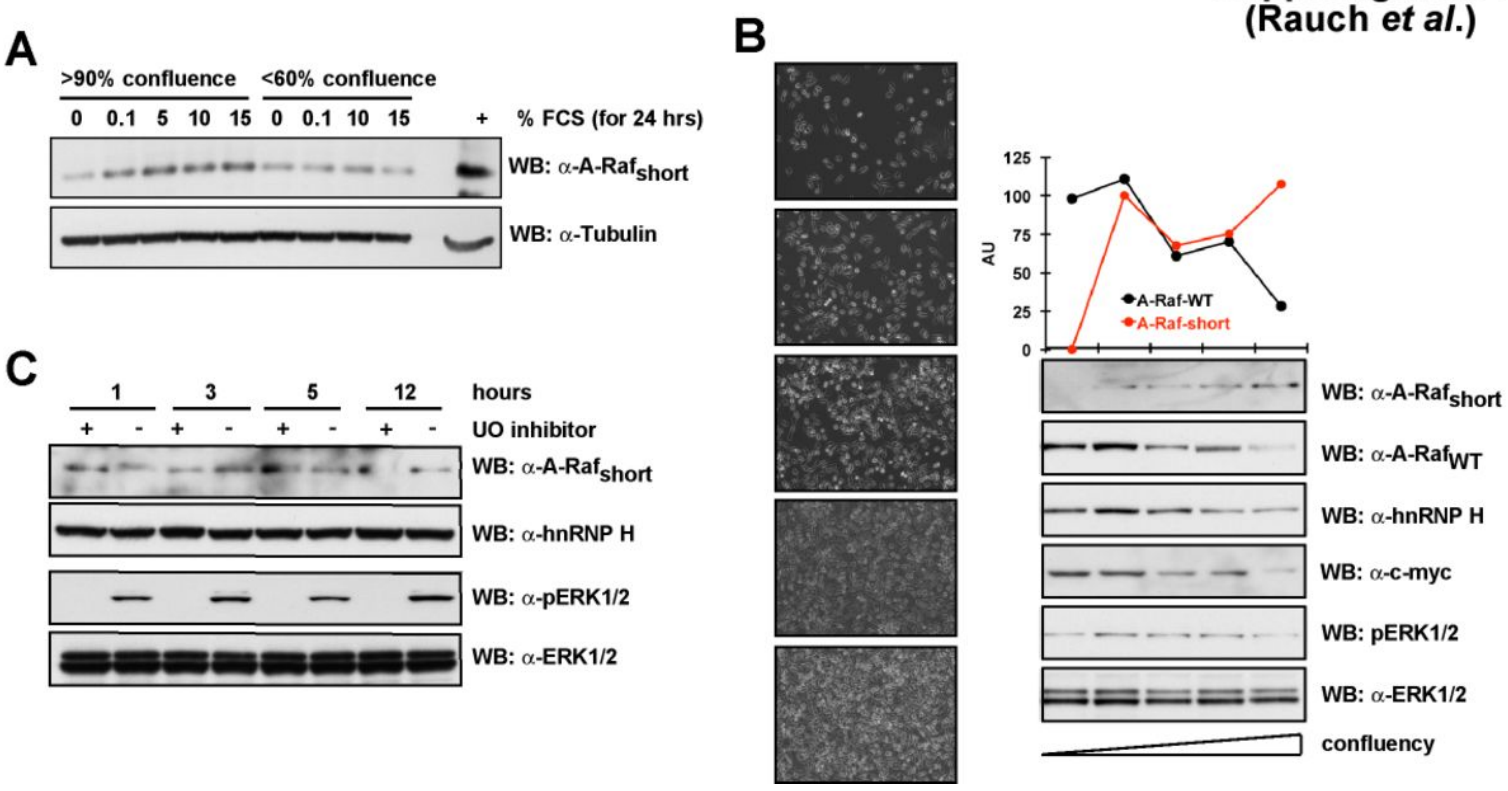

Suppl. Figure S5
(Rauch *et al.*)

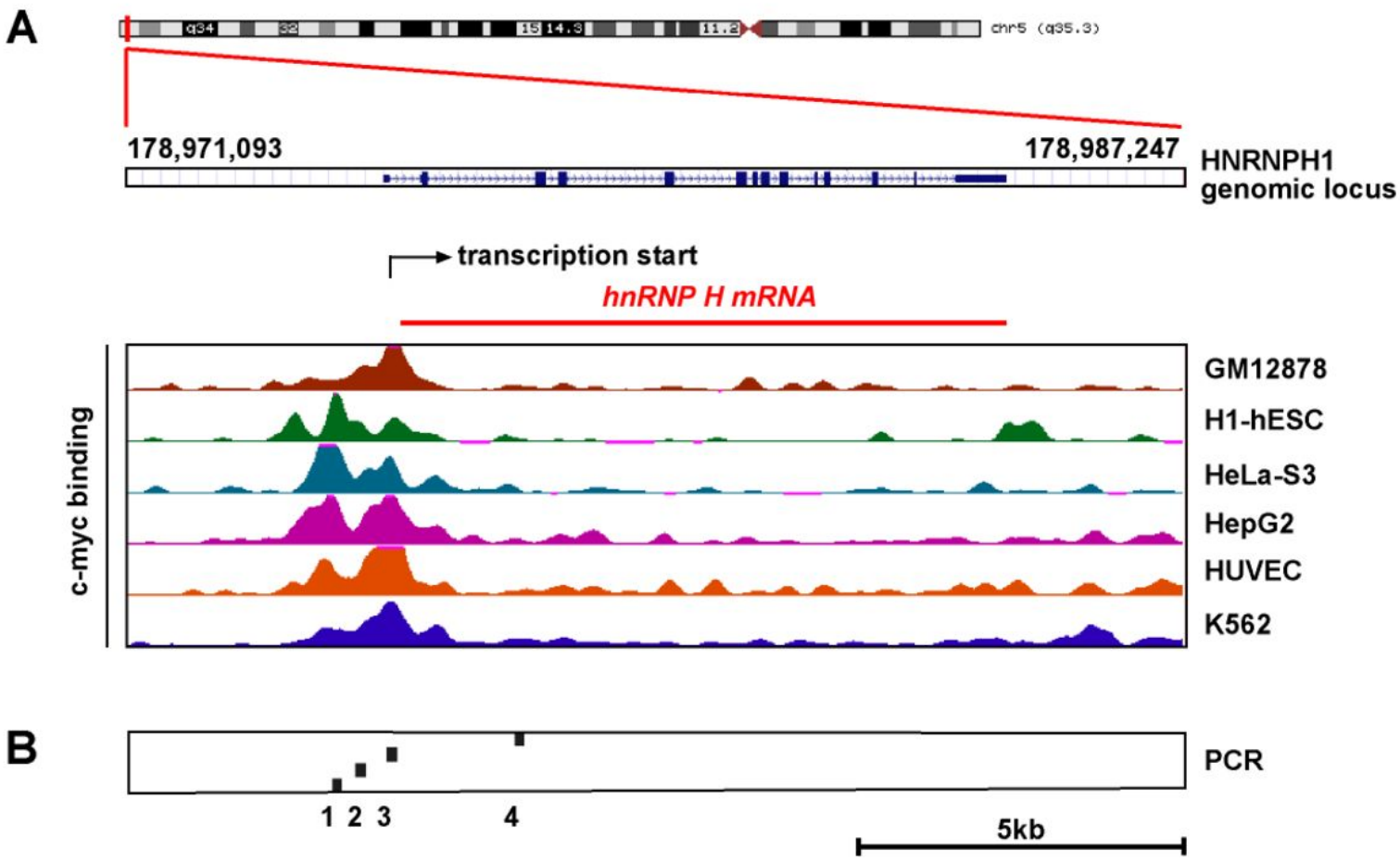

Suppl. Figure S6
(Rauch *et al.*)